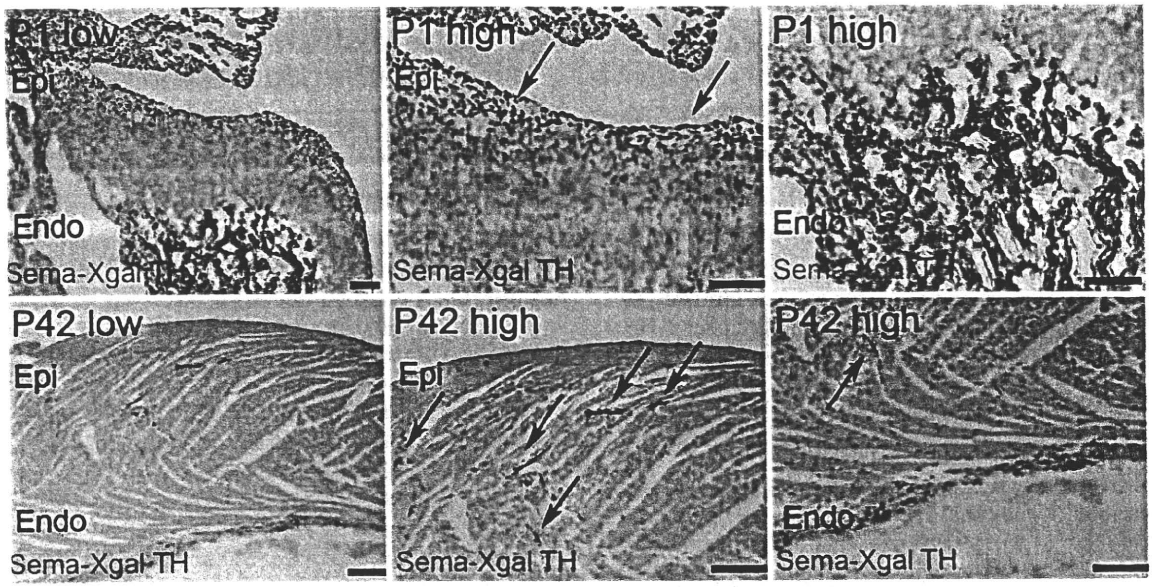

Fig. (3). Inverse expression pattern of *Sema3a* and sympathetic innervation in mouse hearts.
Double staining with TH (brown) and X-gal (blue) in P1 and P42 *Sema3a*$^{lacZ/+}$ hearts. Sympathetic nerves are restricted to the subepicardium at P1, but extend into the myocardium, coincident with downregulation of Sema3a at P42. Scale bar, 100 μm.

SEMA3A DEFICIENT MICE SHOW SINUS ARREST AND SUDDEN DEATH

To investigate whether Sema3a is critical for cardiac sympathetic nerve development, we analyzed *Sema3a*-deficient mice (*Sema3a*$^{-/-}$) [55, 61, 62]. The WT hearts showed a clear epicardial-to-endocardial gradient of sympathetic innervation. By comparison, the sympathetic nerve density was reduced in the subepicardium and enhanced in the subendocardium of *Sema3a*$^{-/-}$ mice, resulting in disruption of the innervation gradient in *Sema3a*$^{-/-}$ ventricles. The *Sema3a*$^{-/-}$ mice also exhibited malformation of the stellate ganglia that extend sympathetic nerves to the heart.

Strikingly, we also found that most of the *Sema3a*$^{-/-}$ mice died within the first postnatal week, with only 20% surviving until weaning [55, 61, 62]. To identify the cause of death and the effects of abnormal sympathetic neural distribution in *Sema3a*$^{-/-}$ hearts, we performed telemetric electrocardiography and heart-rate variability analysis [63, 64]. In addition to multiple premature ventricular contractions, *Sema3a*$^{-/-}$ mice developed sinus bradycardia and abrupt sinus arrest due to sympathetic neural dysfunction (Fig. **4**).

SEMA3A-OVEREXPRESSION CAUSES VENTRICULAR TACHYARRHYTHMIAS DUE TO INNERVATION PATTERNING DEFECTS

We generated transgenic mice that overexpressed *Sema3a* specifically in the heart (*SemaTG*) to determine if the phenotype observed in *Sema3a*$^{-/-}$ hearts is a secondary effect of stellate ganglia malformation [65]. This possibility was discounted as *SemaTG* mice showed reduced sympathetic innervation and attenuation of the epicardial-to-endocardial innervation gradient.

The *SemaTG* mice died suddenly without symptoms at 10 months of age. Sustained ventricular tachyarrhythmia was induced in *SemaTG* mice, but not in WT mice, after epinephrine administration, and programmed electrical stimulation revealed that *SemaTG* mice were highly susceptible to ventricular tachyarrhythmia (Fig. **4** and **5**) [66, 67]. The β1-adrenergic receptor density was upregulated and the cAMP response after catecholamine injection was exaggerated in *SemaTG* ventricles. Action potential duration was significantly prolonged in hypoinnervated *SemaTG* ventricles, presumably via ion channel modulation. These results suggest that the higher susceptibility of *SemaTG* mice to ventricular arrhythmia is due to catecholamine supersensitivity and prolongation of action potential duration, both of which can augment triggered activity in cardiomyocytes [68-72]. Thus, Sema3a-mediated sympathetic innervation patterning is critical for the maintenance of arrhythmia-free hearts.

CONCLUSIONS

Cardiac nerves are highly plastic, and the balance between NGF and Sema3a synthesized in the heart determines cardiac innervation patterning (Fig. **5**). ET-1 upregulates NGF expression in cardiomyocytes, modulates nerve sprouting and plays critical roles in sympathetic nerve development [27, 54]. NGF is also important for sensory innervation, and NGF downregulation may result in silent myocardial ischemia and SCD in diabetic patients [20]. On the other hand, Sema3a inhibits neural growth and establishes appropriate innervation patterning in the heart. Both Sema3a deficiency and overexpression reveal lethal arrhythmias and sudden death due to disruption of sympathetic innervation patterning, suggesting fine tuning of Sema3a is critical for cardiac function. Thus, identification of the

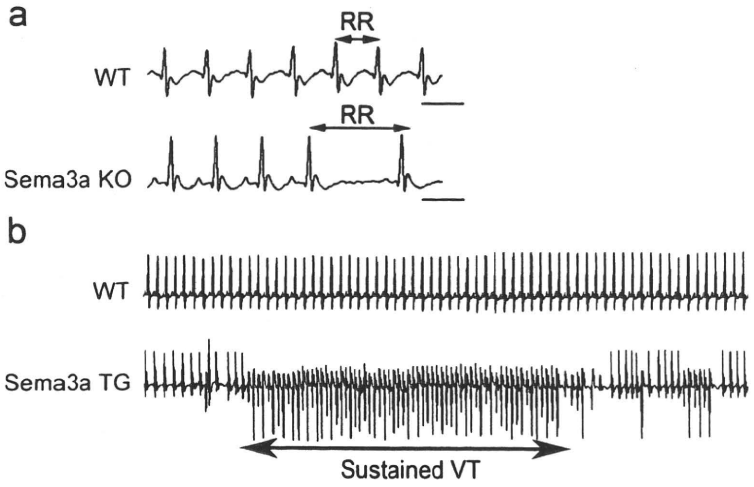

Fig. (4). Various arrhythmias occurred in Sema3a gene-modified mice.
(a) ECG in WT and *Sema3a*$^{-/-}$ mice. Note the abrupt sinus-slowing in *Sema3a*$^{-/-}$ mice. (b) Epinephrine administration revealed sustained VT only in *SemaTG* mice.

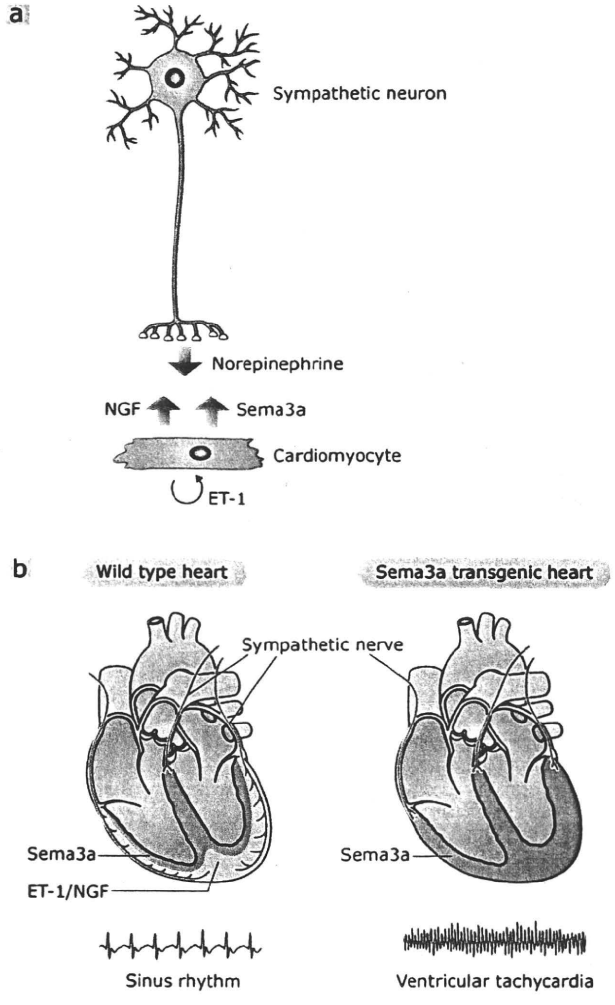

Fig. (5). Cardiac innervation patterning and lethal arrhythmias.
The crosstalk between cardiomyocytes and sympathetic neurons. Neurons synthesize norepinephrine, and cardiomyocytes secret NGF and Sema3a to control cardiac performance. (b) Appropriate Sema3a-mediated sympathetic innervation patterning is critical for the maintenance of an arrhythmia-free heart. *SemaTG* mice are highly susceptible to ventricular tachyarrhythmias.

molecular mechanisms regulating cardiac innervation would improve our general understanding of cardiac performance and disease.

ACKNOWLEDGMENTS

This study was supported in part by research grants from the Ministry of Education, Culture, Sports, Science and Technology, Japan, and the Program for Promotion of Fundamental Studies in Health Sciences of the National Institute of Biomedical Innovation.

REFERENCES

[1] Cao JM, Chen LS, KenKnight BH, *et al.* Nerve sprouting and sudden cardiac death. Circ Res 2000; 86: 816-21.

[2] Kaye DM, Vaddadi G, Gruskin SL, Du XJ, Esler MD. Reduced myocardial nerve growth factor expression in human and experimental heart failure. Circ Res 2000; 86: E80-4.

[3] Cao JM, Fishbein MC, Han JB, *et al.* Relationship between regional cardiac hyperinnervation and ventricular arrhythmia. Circulation 2000; 101: 1960-9.

[4] Chen LS, Zhou S, Fishbein MC, Chen PS. New perspectives on the role of autonomic nervous system in the genesis of arrhythmias. J Cardiovasc Electrophysiol 2007; 18: 123-7.

[5] Chen PS, Chen LS, Cao JM, Sharifi B, Karagueuzian HS, Fishbein MC. Sympathetic nerve sprouting, electrical remodeling and the mechanisms of sudden cardiac death. Cardiovasc Res 2001; 50: 409-16.

[6] Dae MW, Lee RJ, Ursell PC, Chin MC, Stillson CA, Moise NS. Heterogeneous sympathetic innervation in German shepherd dogs with inherited ventricular arrhythmia and sudden cardiac death. Circulation 1997; 96: 1337-42.

[7] Qu J, Robinson RB. Cardiac ion channel expression and regulation: the role of innervation. J Mol Cell Cardiol 2004; 37: 439-48.

[8] Hjalmarson A. Effects of beta blockade on sudden cardiac death during acute myocardial infarction and the postinfarction period. Am J Cardiol 1997; 80: 35J-9J.

[9] Poole-Wilson PA, Swedberg K, Cleland JG, *et al.* Comparison of carvedilol and metoprolol on clinical outcomes in patients with chronic heart failure in the Carvedilol Or Metoprolol European Trial (COMET): randomised controlled trial. Lancet 2003; 362: 7-13.

[10] Faerman I, Faccio E, Milei J, *et al.* Autonomic neuropathy and painless myocardial infarction in diabetic patients. Histologic evidence of their relationship. Diabetes 1977; 26: 1147-58.

[11] Crowley C, Spencer SD, Nishimura MC, *et al.* Mice lacking nerve growth factor display perinatal loss of sensory and sympathetic

neurons yet develop basal forebrain cholinergic neurons. Cell 1994; 76: 1001-11.
[12] Ito M, Zipes DP. Efferent sympathetic and vagal innervation of the canine right ventricle. Circulation 1994; 90: 1459-68.
[13] Crick SJ, Sheppard MN, Ho SY, Anderson RH. Localisation and quantitation of autonomic innervation in the porcine heart I: conduction system. J Anat 1999; 195: 341-57.
[14] Crick SJ, Wharton J, Sheppard MN, *et al.* Innervation of the human cardiac conduction system. A quantitative immunohistochemical and histochemical study. Circulation 1994; 89: 1697-708.
[15] Chow LT, Chow SS, Anderson RH, Gosling JA. Innervation of the human cardiac conduction system at birth. Br Heart J 1993; 69: 430-5.
[16] Hansson M, Kjorell U, Forsgren S. Increased immunoexpression of atrial natriuretic peptide in the heart conduction system of the rat after cardiac sympathectomy. J Mol Cell Cardiol 1998; 30: 2047-57.
[17] Randall WC, Szentivanyi M, Pace JB, Wechsler JS, Kaye MP. Patterns of sympathetic nerve projections onto the canine heart. Circ Res 1968; 22: 315-23.
[18] Schultz HD, Ustinova EE. Capsaicin receptors mediate free radical-induced activation of cardiac afferent endings. Cardiovasc Res 1998; 38: 348-55.
[19] Hua F, Harrison T, Qin C, *et al.* c-Fos expression in rat brain stem and spinal cord in response to activation of cardiac ischemia-sensitive afferent neurons and electrostimulatory modulation. Am J Physiol Heart Circ Physiol 2004; 287: H2728-38.
[20] Ieda M, Kanazawa H, Ieda Y, *et al.* Nerve growth factor is critical for cardiac sensory innervation and rescues neuropathy in diabetic hearts. Circulation 2006; 114: 2351-63.
[21] Snider WD. Functions of the neurotrophins during nervous system development: what the knockouts are teaching us. Cell 1994; 77: 627-38.
[22] Lockhart ST, Turrigiano GG, Birren SJ. Nerve growth factor modulates synaptic transmission between sympathetic neurons and cardiac myocytes. J Neurosci 1997; 17: 9573-82.
[23] Brennan C, Rivas-Plata K, Landis SC. The p75 neurotrophin receptor influences NT-3 responsiveness of sympathetic neurons *in vivo*. Nat Neurosci 1999; 2: 699-705.
[24] Heumann R, Korsching S, Scott J, Thoenen H. Relationship between levels of nerve growth factor (NGF) and its messenger RNA in sympathetic ganglia and peripheral target tissues. EMBO J 1984; 3: 3183-9.
[25] Kanki H, Fukuda K, Okushi K, *et al.* Comparison of nerve growth factor mRNA expression in cardiac and skeletal muscle in streptozotocin-induced diabetic mice. Life Sci 1999; 65: 2305-13.
[26] Zhou S, Chen LS, Miyauchi Y, *et al.* Mechanisms of cardiac nerve sprouting after myocardial infarction in dogs. Circ Res 2004; 95: 76-83.
[27] Kimura K, Ieda M. Kanazawa H, *et al.* Cardiac sympathetic rejuvenation: a link between nerve function and cardiac hypertrophy. Circ Res 2007; 100: 1755-64.
[28] Kuo DC, Oravitz JJ, DeGroat WC. Tracing of afferent and efferent pathways in the left inferior cardiac nerve of the cat using retrograde and transganglionic transport of horseradish peroxidase. Brain Res 1984; 321: 111-8.
[29] Zahner MR, Li DP, Chen SR, Pan HL. Cardiac vanilloid receptor 1-expressing afferent nerves and their role in the cardiogenic sympathetic reflex in rats. J Physiol 2003; 551: 515-23.
[30] Bennett DL, Dmietrieva N, Priestley JV, Clary D, McMahon SB. trkA, CGRP and IB4 expression in retrogradely labelled cutaneous and visceral primary sensory neurones in the rat. Neurosci Lett 1996; 206: 33-6.
[31] Trupp M, Ryden M, Jornvall H, *et al.* Peripheral expression and biological activities of GDNF, a new neurotrophic factor for avian and mammalian peripheral neurons. J Cell Biol 1995; 130: 137-48.
[32] Kuruvilla R, Zweifel LS, Glebova NO, *et al.* A neurotrophin signaling cascade coordinates sympathetic neuron development through differential control of TrkA trafficking and retrograde signaling. Cell 2004; 118: 243-55.
[33] Wang L, Wang DH. TRPV1 gene knockout impairs postischemic recovery in isolated perfused heart in mice. Circulation 2005; 112: 3617-23.
[34] Pan HL, Chen SR. Sensing tissue ischemia: another new function for capsaicin receptors? Circulation 2004; 110: 1826-31.
[35] Park AM, Armin S, Azarbal A, Lai A, Chen PS, Fishbein MC. Distribution of cardiac nerves in patients with diabetes mellitus: an immunohistochemical postmortem study of human hearts. Cardiovasc Pathol 2002; 11: 326-31.
[36] Schratzberger P, Walter DH, Rittig K, *et al.* Reversal of experimental diabetic neuropathy by VEGF gene transfer. J Clin Invest 2001; 107: 1083-92.
[37] Fernyhough P, Diemel LT, Hardy J, Brewster WJ, Mohiuddi L, Tomlinson DR. Human recombinant nerve growth factor replaces deficient neurotrophic support in the diabetic rat. Eur J Neurosci 1995; 7: 1107-10.
[38] Christianson JA, Riekhof JT, Wright DE. Restorative effects of neurotrophin treatment on diabetes-induced cutaneous axon loss in mice. Exp Neurol 2003; 179: 188-99.
[39] Unger JW, Klitzsch T, Pera S, Reiter R. Nerve growth factor (NGF) and diabetic neuropathy in the rat: morphological investigations of the sural nerve, dorsal root ganglion, and spinal cord. Exp Neurol 1998; 153: 23-34.
[40] Bierhaus A, Haslbeck KM, Humpert PM, *et al.* Loss of pain perception in diabetes is dependent on a receptor of the immunoglobulin superfamily. J Clin Invest 2004; 114: 1741-51.
[41] Feldman EL, Russell JW, Sullivan KA, Golovoy D. New insights into the pathogenesis of diabetic neuropathy. Curr Opin Neurol 1999; 12: 553-63.
[42] Emanueli C, Salis MB, Pinna A, Graiani G, Manni L, Madeddu P. Nerve growth factor promotes angiogenesis and arteriogenesis in ischemic hindlimbs. Circulation 2002; 106: 2257-62.
[43] Hellweg R, Hartung HD. Endogenous levels of nerve growth factor (NGF) are altered in experimental diabetes mellitus: a possible role for NGF in the pathogenesis of diabetic neuropathy. J Neurosci Res 1990; 26: 258-67.
[44] Schmid H, Forman LA, Cao X, Sherman PS, Stevens MJ. Heterogeneous cardiac sympathetic denervation and decreased myocardial nerve growth factor in streptozotocin-induced diabetic rats: implications for cardiac sympathetic dysinnervation complicating diabetes. Diabetes 1999; 48: 603-8.
[45] Hellweg R, Raivich G, Hartung HD, Hock C, Kreutzberg GW. Axonal transport of endogenous nerve growth factor (NGF) and NGF receptor in experimental diabetic neuropathy. Exp Neurol 1994; 130: 24-30.
[46] Futamatsu H, Suzuki J, Mizuno S, *et al.* Hepatocyte growth factor ameliorates the progression of experimental autoimmune myocarditis: a potential role for induction of T helper 2 cytokines. Circ Res 2005; 96: 823-30.
[47] Sakata K, Kumagai H, Osaka M, *et al.* Potentiated sympathetic nervous and renin-angiotensin systems reduce nonlinear correlation between sympathetic activity and blood pressure in conscious spontaneously hypertensive rats. Circulation 2002; 106: 620-5.
[48] Apfel SC, Schwartz S, Adornato BT, *et al.* Efficacy and safety of recombinant human nerve growth factor in patients with diabetic polyneuropathy: A randomized controlled trial. rhNGF Clinical Investigator Group. JAMA 2000; 284: 2215-21.
[49] Goss JR, Goins WF, Lacomis D, Mata M, Glorioso JC, Fink DJ. Herpes simplex-mediated gene transfer of nerve growth factor protects against peripheral neuropathy in streptozotocin-induced diabetes in the mouse. Diabetes 2002; 51: 2227-32.
[50] Sasaki K, Chancellor MB, Goins WF, *et al.* Gene therapy using replication-defective herpes simplex virus vectors expressing nerve growth factor in a rat model of diabetic cystopathy. Diabetes 2004; 53: 2723-30.
[51] Zhan Y, Kim S, Izumi Y, *et al.* Role of JNK, p38, and ERK in platelet-derived growth factor-induced vascular proliferation, migration, and gene expression. Arterioscler Thromb Vasc Biol 2003; 23: 795-801.
[52] Francis N, Farinas I, Brennan C, *et al.* NT-3, like NGF, is required for survival of sympathetic neurons, but not their precursors. Dev Biol 1999; 210: 411-27.
[53] Hassankhani A, Steinhelper ME, Soonpaa MH, *et al.* Overexpression of NGF within the heart of transgenic mice causes hyperinnervation, cardiac enlargement, and hyperplasia of ectopic cells. Dev Biol 1995; 169: 309-21.
[54] Ieda M, Fukuda K, Hisaka Y, *et al.* Endothelin-1 regulates cardiac sympathetic innervation in the rodent heart by controlling nerve growth factor expression. J Clin Invest 2004; 113: 876-84.

[55] Ieda M, Kanazawa H, Kimura K, *et al.* Sema3a maintains normal heart rhythm through sympathetic innervation patterning. Nat Med 2007; 13: 604-12.

[56] Puschel AW, Adams RH, Betz H. Murine semaphorin D/collapsin is a member of a diverse gene family and creates domains inhibitory for axonal extension. Neuron 1995; 14: 941-8.

[57] Tanelian DL, Barry MA, Johnston SA, Le T, Smith GM. Semaphorin III can repulse and inhibit adult sensory afferents *in vivo*. Nat Med 1997; 3: 1398-401.

[58] Kawasaki T, Bekku Y, Suto F, *et al.* Semaphorin III can repulse and inhibit adult sensory afferents *in vivo*. Development 2002; 129: 671-80.

[59] Tago H, Kimura H, Maeda T. Visualization of detailed acetylcholinesterase fiber and neuron staining in rat brain by a sensitive histochemical procedure. J Histochem Cytochem 1986; 34: 1431-8.

[60] Kupershmidt S, Yang T, Anderson ME, *et al.* Replacement by homologous recombination of the minK gene with lacZ reveals restriction of minK expression to the mouse cardiac conduction system. Circ Res 1999; 84: 146-52.

[61] Behar O, Golden JA, Mashimo H, Schoen FJ, Fishman MC. Semaphorin III is needed for normal patterning and growth of nerves, bones and heart. Nature 1996; 383: 525-8.

[62] Taniguchi M, Yuasa S, Fujisawa H, *et al.* Disruption of semaphorin III/D gene causes severe abnormality in peripheral nerve projection. Neuron 1997; 19: 519-30.

[63] Shusterman V, Usiene I, Harrigal C, *et al.* Strain-specific patterns of autonomic nervous system activity and heart failure susceptibility in mice. Am J Physiol Heart Circ Physiol 2002; 282: H2076-83.

[64] Saba S, London B, Ganz L. Autonomic blockade unmasks maturational differences in rate-dependent atrioventricular nodal conduction and facilitation in the mouse. J Cardiovasc Electrophysiol 2003; 14: 191-5.

[65] Gulick J, Subramaniam A, Neumann J, Robbins J. Isolation and characterization of the mouse cardiac myosin heavy chain genes. J Biol Chem 1991; 266: 9180-5.

[66] Wehrens XH, Lehnart SE, Reiken SR, *et al.* Protection from cardiac arrhythmia through ryanodine receptor-stabilizing protein calstabin2. Science 2004; 304: 292-6.

[67] Kannankeril PJ, Mitchell BM, Goonasekera SA, *et al.* Mice with the R176Q cardiac ryanodine receptor mutation exhibit catecholamine-induced ventricular tachycardia and cardiomyopathy. Proc Natl Acad Sci U S A 2006; 103: 12179-84.

[68] Kuo HC, Cheng CF, Clark RB, *et al.* A defect in the Kv channel-interacting protein 2 (KChIP2) gene leads to a complete loss of I(to) and confers susceptibility to ventricular tachycardia. Cell 2001; 107: 801-13.

[69] Opthof T, Misier AR, Coronel R, *et al.* Dispersion of refractoriness in canine ventricular myocardium. Effects of sympathetic stimulation. Circ Res 1991; 68: 1204-15.

[70] Priori SG, Corr PB. Mechanisms underlying early and delayed afterdepolarizations induced by catecholamines. Am J Physiol 1990; 258: H1796-805.

[71] Brunet S, Aimond F, Li H, *et al.* Heterogeneous expression of repolarizing, voltage-gated K+ currents in adult mouse ventricles. J Physiol 2004; 559: 103-20.

[72] Costantini DL, Arruda EP, Agarwal P, *et al.* The homeodomain transcription factor Irx5 establishes the mouse cardiac ventricular repolarization gradient. Cell 2005; 123: 347-58.

Received: October 6, 2008 Revised: February 28, 2009 Accepted: March 10, 2009

Glucocorticoid protects rodent hearts from ischemia/reperfusion injury by activating lipocalin-type prostaglandin D synthase–derived PGD_2 biosynthesis

Satori Tokudome,[1,2] Motoaki Sano,[1,3] Ken Shinmura,[4] Tomohiro Matsuhashi,[1,5] Shintaro Morizane,[1,6] Hidenori Moriyama,[1] Kayoko Tamaki,[4] Kentaro Hayashida,[1,5] Hiroki Nakanishi,[7] Noritada Yoshikawa,[8] Noriaki Shimizu,[8] Jin Endo,[1,5] Takaharu Katayama,[1,5] Mitsushige Murata,[1,5] Shinsuke Yuasa,[1,5] Ruri Kaneda,[1] Kengo Tomita,[9] Naomi Eguchi,[10] Yoshihiro Urade,[10] Koichiro Asano,[11] Yasunori Utsunomiya,[2] Takeshi Suzuki,[6] Ryo Taguchi,[7] Hirotoshi Tanaka,[8] and Keiichi Fukuda[1]

[1]Department of Regenerative Medicine and Advanced Cardiac Therapeutics, School of Medicine, Keio University, Tokyo, Japan. [2]Division of Kidney and Hypertension, Department of Internal Medicine, Jikei University School of Medicine, Tokyo, Japan. [3]Precursory Research for Embryonic Science and Technology (PRESTO), Japan Science and Technology Agency, Tokyo, Japan. [4]Division of Geriatric Medicine and [5]Division of Cardiology, School of Medicine, and [6]Division of Basic Biological Sciences, Faculty of Pharmacy, Keio University, Tokyo, Japan. [7]Department of Metabolomics and [8]Division of Clinical Immunology, Advanced Clinical Research Center, and Department of Rheumatology and Allergy, Research Hospital, Institute of Medical Science, University of Tokyo, Tokyo, Japan. [9]Division of Gastroenterology, Department of Internal Medicine, School of Medicine, Keio University, Tokyo, Japan. [10]Department of Molecular and Behavioral Biology, Osaka Bioscience Institute, Osaka, Japan. [11]Division of Pulmonary Medicine, School of Medicine, Keio University, Tokyo, Japan.

Lipocalin-type prostaglandin D synthase (L-PGDS), which was originally identified as an enzyme responsible for PGD_2 biosynthesis in the brain, is highly expressed in the myocardium, including in cardiomyocytes. However, the factors that control expression of the gene encoding L-PGDS and the pathophysiologic role of L-PGDS in cardiomyocytes are poorly understood. In the present study, we demonstrate that glucocorticoids, which act as repressors of prostaglandin biosynthesis in most cell types, upregulated the expression of L-PGDS together with cytosolic calcium-dependent phospholipase A2 and COX2 via the glucocorticoid receptor (GR) in rat cardiomyocytes. Accordingly, PGD_2 was the most prominently induced prostaglandin in vivo in mouse hearts and in vitro in cultured rat cardiomyocytes after exposure to GR-selective agonists. In isolated Langendorff-perfused mouse hearts, dexamethasone alleviated ischemia/reperfusion injury. This cardioprotective effect was completely abrogated by either pharmacologic inhibition of COX2 or disruption of the gene encoding L-PGDS. In in vivo ischemia/reperfusion experiments, dexamethasone reduced infarct size in wild-type mice. This cardioprotective effect of dexamethasone was markedly reduced in L-PGDS–deficient mice. In cultured rat cardiomyocytes, PGD_2 protected against cell death induced by anoxia/reoxygenation via the D-type prostanoid receptor and the ERK1/2-mediated pathway. Taken together, these results suggest what we believe to be a novel interaction between glucocorticoid-GR signaling and the cardiomyocyte survival pathway mediated by the arachidonic acid cascade.

Introduction

Glucocorticoids play a key role in the response to stress, influencing the regulation of blood pressure, inflammation, immune function, and cellular energy metabolism (1). These acute effects contribute to an adaptive response, at least in the short term. For example, the cardioprotective effects of glucocorticoids in the acute setting of myocardial ischemia/reperfusion have been experimentally demonstrated in animals (2–5) and in humans (6). The beneficial effect of glucocorticoids has been attributed mostly to their ability to limit the acute inflammatory response associated with acute myocardial infarction: glucocorticoids act on leukocytes and endothelial cells to attenuate leukocyte-endothelial cell interactions (7) and to reduce the generation and release of proinflammatory cytokines and mediators (8). Alternatively, acute induction of endothelial nitric oxide synthase, possibly through nongenomic effects of the glucocorticoid receptor (GR) on endothelial cells, may reduce tissue injury caused by ischemia/reperfusion (9). However, little is known regarding the genomic actions of glucocorticoids on cardiomyocytes.

The GR is a member of the nuclear receptor superfamily of ligand-dependent transcription factors that positively and negatively regulate gene expression by distinct mechanisms (10). In the absence of glucocorticoids, the GR is sequestered in the cytoplasm by a protein complex that includes heat shock proteins. Upon

Conflict of interest: The authors have declared that no conflict of interest exists

Nonstandard abbreviations used: ALD, aldosterone; COR, corticosterone; cPLA2, cytosolic calcium-dependent phospholipase A2; CRTH2, chemoattractant receptor-like molecule expressed on Th2 cells; CVZ, cortivazol; DEX, dexamethasone; DP, D-type prostanoid; $+dP/dt$, positive LV peak dP/dt; GR, glucocorticoid receptor; H-PGDS, hematopoietic-type prostaglandin D_2 synthase; LC-MS/MS, liquid chromatography–mass spectrometry/mass spectrometry; L-PGDS, lipocalin-type prostaglandin D synthase; LVDP, LV developed pressure; LVEDP, LV end-diastolic pressure; MR, mineralocorticoid receptor; Q-PCR, real-time quantitative PCR.

Citation for this article: *J. Clin. Invest.* **119**:1477–1488 (2009) doi:10.1172/JCI37413

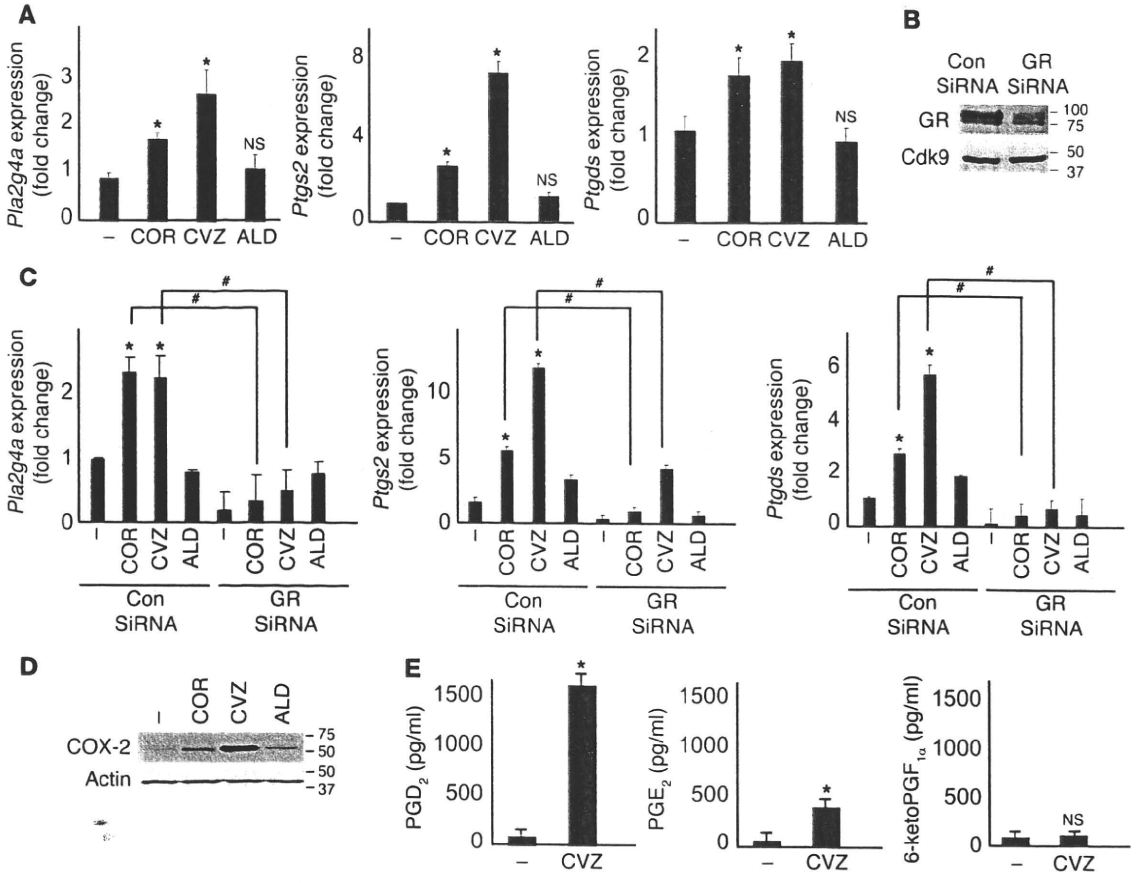

Figure 1

Glucocorticoids positively regulate PGD_2 biosynthesis by stimulating the expression of *Ptgs2*, *Pla2g4a*, and *Ptgds* via the GR in neonatal cardiomyocytes. (**A**) Neonatal rat cardiomyocytes were treated with vehicle (–) or with 100 nM COR, CVZ, or ALD for 3 hours. RNA was extracted, and Q-PCR was performed to determine the mRNA levels of *Ptgs2*, *Pla2g4a*, and *Ptgds* ($n = 5$). (**B**) Neonatal rat cardiomyocytes were transfected with control (Con) or GR siRNA. The endogenous GR protein levels were determined by Western blotting. (**C**) Control or GR siRNA–treated cells were treated with vehicle or stimulated with 100 nM COR, CVZ, or ALD for 3 hours. The mRNA levels of *Pla2g4a*, *Ptgs2*, and *Ptgds* were examined by Q-PCR ($n = 5$). (**D**) Neonatal rat cardiomyocytes were treated with vehicle or with 100 nM COR, CVZ, or ALD for 24 hours, and COX2 protein levels were determined by Western blotting. The membranes were stripped and reprobed with anti–α-actin antibodies. (**E**) Neonatal rat cardiomyocytes were treated with vehicle or 100 nM CVZ for 48 hours. The culture media were subjected to ELISA to quantify prostaglandin production from the cardiomyocytes ($n = 5$). $^*P < 0.05$ versus vehicle; $^\#P < 0.05$; Student's *t* test.

glucocorticoid binding, GR is released from this inactive complex and translocates to the nucleus. Within the nucleus, ligand-bound GR binds to palindromic glucocorticoid-responsive elements in specific promoters, thereby activating the transcription of target genes. In contrast, the GR suppresses the activation of inflammatory response genes by interfering with the activities of signal-dependent transcription factors, such as activator protein-1 and nuclear factor-κB (11, 12). This activity, which is referred to as transrepression, accounts for most of the antiinflammatory actions of glucocorticoids (10).

The elucidation of tissue-specific target genes of GR action is difficult, since the GR overlaps functionally with the mineralocorticoid receptor (MR) at the level of ligand-binding specificity, and most metabolically active organs, including the heart, express substantial levels of both GR and MR. Endogenous glucocorticoid – namely, cortisol in humans and corticosterone (COR) in rodents – binds to both the GR and the MR with comparable affinity (13). In the absence of 11β-hydroxysteroid dehydrogenase 2, which converts the glucocorticoid to inactive metabolites, the intramyocardial concentration of glucocorticoid reflects the free concentration in plasma, which is 1,000-fold higher than that of the mineralocorticoid aldosterone (ALD). Therefore, it seems likely that glucocorticoid rather than mineralocorticoid occupies the MR and influences the proinflammatory response after myocardial infarction (14). Thus, it is crucial to clarify the GR-specific target genes independently of the functional redundancy with MR.

Recently, we performed DNA microarray analysis to evaluate the changes in gene expression profiles in neonatal rat cardiomyocytes after stimulation with COR, the GR-selective agonist cortivazol (CVZ; refs. 15, 16), or ALD (17). Unexpectedly, we found that the expression of genes that encode 2 key enzymes in a common pathway of prostaglandin biosynthesis were upregulated by glucocorticoids via the GR in cardiomyocytes: phospholipase A2 group IVA (*Pla2g4a*; encoding cytosolic calcium-dependent phospholipase A2 [cPLA2]), which belongs to the class of cPLA2s that preferentially cleave arachidonic acid from membrane phospholipids; and pros-

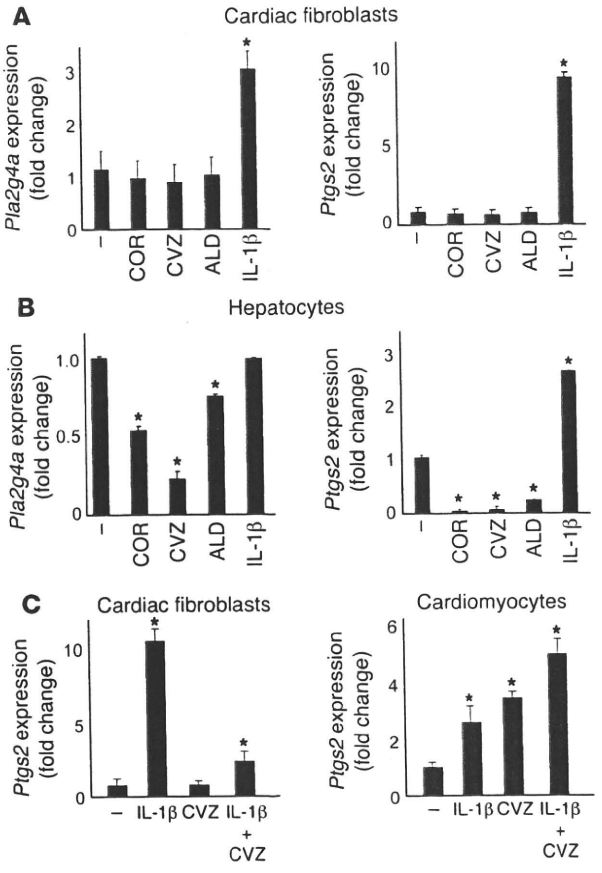

Figure 2

Glucocorticoids stimulate or suppress *Pla2g4a* and *Ptgs2* expression in a cell type–specific manner. (**A** and **B**) Neonatal rat fibroblasts (**A**) and adult mouse hepatocytes (**B**) were treated with vehicle; with 100 nM COR, CVZ, or ALD; or with 10 ng/μl IL-1β for 3 hours. The expression levels of the indicated genes were determined by Q-PCR ($n = 5$). (**C**) Neonatal rat cardiac fibroblasts and cardiomyocytes were treated with vehicle or were stimulated with 10 ng/μl IL-1β, 100 nM CVZ, or the combination for 3 hours. The expression levels of the indicated genes were determined by Q-PCR ($n = 5$). $^*P < 0.05$ versus vehicle; Student's *t* test.

taglandin-endoperoxide synthase 2 (*Ptgs2*; encoding COX2), which converts arachidonic acid into PGH_2. Importantly, ALD did not have similar stimulatory effects on these genes. The induction of *Pla2g4a* and *Ptgs2* by GR is specific for cardiomyocytes, since GR has been shown to transrepress the activation of these proinflammatory genes in most cells (1). Therefore, we sought to investigate the major types of prostanoids produced in cardiomyocytes after exposure to glucocorticoids and to clarify the roles of these products in cardiac physiology. Among the genes for PGH_2 isomerases, expression of *Ptgds*, which encodes lipocalin-type prostaglandin D synthase (L-PGDS), was selectively upregulated by a GR-specific ligand. Consistent with this result, PGD_2 was the most prominently induced prostaglandin by GR-specific ligand stimulation of cultured cardiomyocytes and in vivo hearts. Using isolated Langendorff-perfused hearts and cultured cardiomyocytes, we demonstrate that the activation of L-PGDS–mediated production of PGD_2 was crucial for the cardioprotection against ischemia/reperfusion conferred by glucocorticoid-GR signaling. Our results suggest what we believe to be a novel interaction between glucocorticoid-GR signaling and the arachidonic acid cascade-mediated cardiomyocyte survival pathway.

Results

Glucocorticoid-GR signaling positively regulates PGD_2 synthesis via the induction of Pla2g4a, Ptgs2, and Ptgds in neonatal rat cardiomyocytes. Based on the microarray analysis, we identified 3 key GR-selective target genes involved in PGD_2 biosynthesis in cardiomyocytes: *Pla2g4a*, *Ptgs2*, and *Ptgds*. Their induction in cultured cardiomyocytes was validated by real-time quantitative PCR (Q-PCR) analysis. Treatment with COR and CVZ, but not ALD, increased the levels of *Pla2g4a*, *Ptgs2*, and *Ptgds* transcripts (Figure 1A). The siRNA-mediated knockdown of GR completely blocked the induction of *Pla2g4a*, *Ptgs2*, and *Ptgds* transcripts by COR or CVZ (Figure 1, B and C). Western blotting demonstrated that both CVZ and COR induced COX2 expression at the protein level, while ALD had little effect on COX2 expression (Figure 1D). Next, we stimulated cultured cardiomyocytes with CVZ for 24 hours and measured the prostaglandin concentrations in the culture media by ELISA. CVZ mainly stimulated the production of PGD_2. CVZ also increased the production of PGE_2 by cultured neonatal rat cardiomyocytes, albeit to a lower level, and had no effect on the production of the PGI_2 metabolite 6-keto-$PGF_{1\alpha}$ (Figure 1E).

The GR-mediated positive transcriptional regulation of *Pla2g4a* and *Ptgs2* was cardiomyocyte specific, since the expression levels of these genes were not affected in cardiac fibroblasts (Figure 2A), but were suppressed in adult hepatocytes (Figure 2B). In contrast, glucocorticoids stimulated serum glucocorticoid–regulated kinase (*Sgk*) expression in all the cell types examined (data not shown).

Glucocorticoid stimulates Pla2g4a and Ptgs2 expression in cardiomyocytes, even in the presence of proinflammatory stimuli. We examined the impact of glucocorticoids on *Ptgs2* expression in the presence of proinflammatory stimuli. The proinflammatory cytokine IL-1β markedly induced *Ptgs2* expression in both cardiac fibroblasts and cardiomyocytes. Costimulation with CVZ suppressed IL-1β–mediated induction of *Ptgs2* in cardiac fibroblasts. In contrast, costimulation with CVZ increased IL-1β–induced *Ptgs2* expression in cardiomyocytes (Figure 2C). These findings indicate that CVZ promotes *Ptgs2* expression in cardiomyocytes at both the basal level and in the presence of proinflammatory cytokine stimulation.

Glucocorticoids stimulate the production of PGD_2 in the adult heart. To directly determine the changes in arachidonic acid metabolism brought about by glucocorticoid-GR signaling in adult hearts, mice were injected i.p. with dexamethasone (DEX) at 2 mg/kg. Q-PCR analysis revealed that the levels of *Pla2g4a*, *Ptgs2*, and *Ptgds* transcripts in adult hearts at 6 hours after DEX administration increased 7.5-, 2.3-, and 1.8-fold, respectively, compared with vehicle-treated hearts (Figure 3A). RU486 injected i.p. 1 hour before DEX injection blocked DEX-mediated induction of these genes. Western blot analysis showed that the protein levels of L-PGDS increased 24 hours after DEX administration in an RU486-sensitive manner (Figure 3B). Another PGD synthase, hematopoietic-type prostaglandin D_2 synthase (H-PGDS), was also expressed in the hearts, although the H-PGDS protein levels were not affected by DEX treatment. DEX administration had no effect on the levels of COX1, microsomal PGE synthase-1 (mPGES-1), mPGES-2, and cytosolic PGE synthase (Supplemental Figure 1; supplemental material available online with this

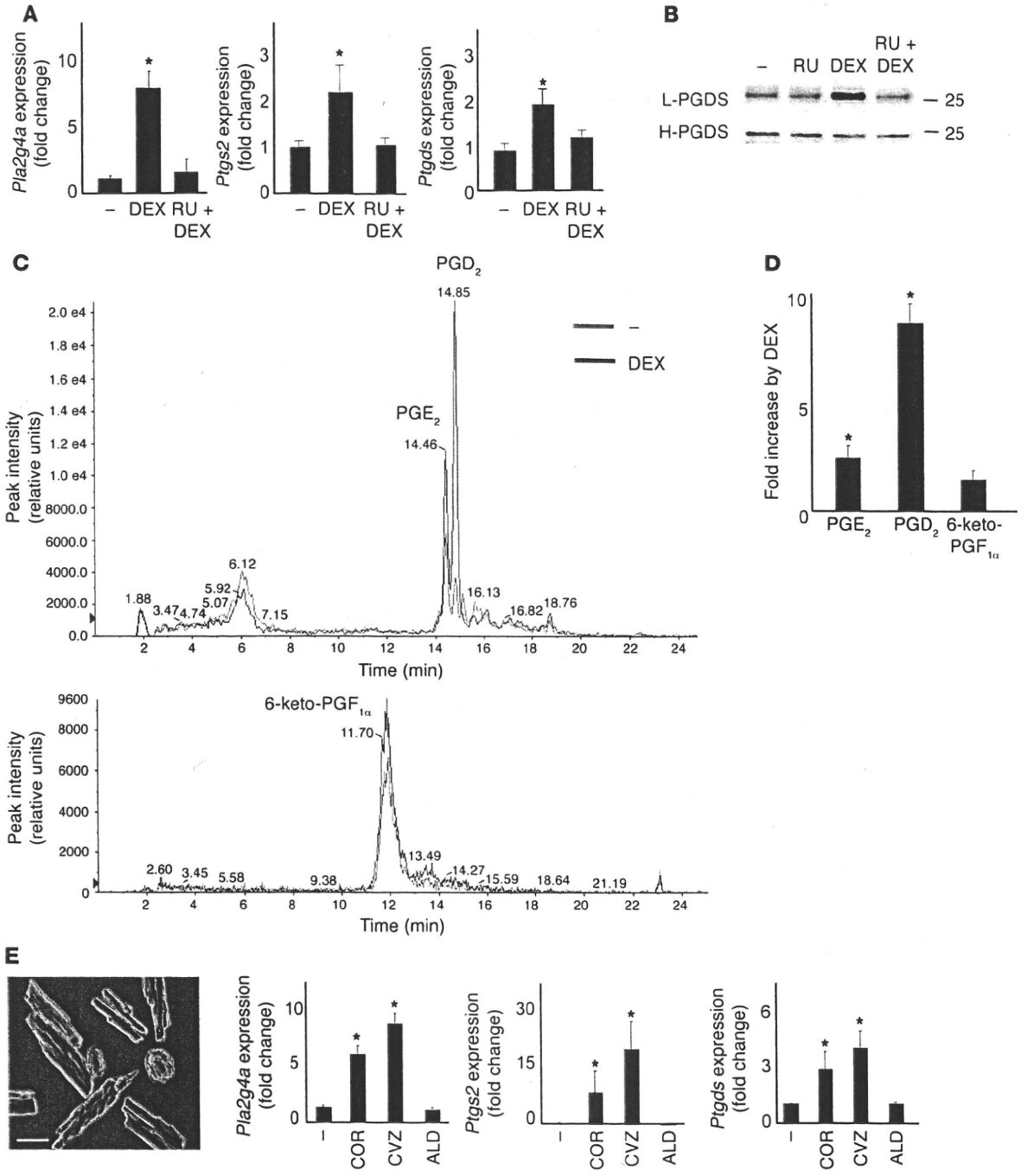

Figure 3

Glucocorticoids stimulate PGD_2 synthesis in adult hearts. (**A**) Adult 12-week-old male mice were injected i.p. with DEX at 2 mg/kg. RU486 (RU; 20 mg/kg) was injected 1 hour before DEX injection. The levels of induction of *Pla2g4a*, *Ptgs2*, and *Ptgds* expression in the ventricular myocardium were determined by Q-PCR ($n = 5$). (**B**) L-PGDS and H-PGDS protein levels were determined by Western blotting. (**C**) Levels of cardiac prostaglandins in vehicle- or DEX-injected mice were analyzed by LC-MS/MS. Representative results are shown; experiments were repeated 3 times. (**D**) Quantification of intramyocardial prostaglandins ($n = 3$). (**E**) Adult mouse cardiomyocytes were prepared and treated with vehicle or with 100 nM COR, CVZ, or ALD for 3 hours. Shown is a representative image of the cardiomyocyte culture. Scale bar: 20 μm. RNA was extracted, and Q-PCR was performed to determine the mRNA levels of *Ptgs2*, *Pla2g4a*, and *Ptgds* ($n = 5$). *$P < 0.05$ versus vehicle; Student's *t* test.

article; doi:10.1172/JCI37413DS1). In line with the induction of these enzymes, quantitative analysis of oxidative arachidonic acid metabolites by liquid chromatography–mass spectrometry/mass spectrometry (LC-MS/MS; ref. 18) demonstrated a 6.2-fold increase in the level of intramuscular PGD_2 in DEX-treated compared with vehicle-treated hearts (Figure 3, C and D). DEX also increased the PGE_2 level 1.8-fold, whereas it had no effect on the level of 6-keto-$PGF_{1\alpha}$. However, we need to use caution when inter-

Table 1
Cardiac parameters before the induction of ischemia

	LVSP (mmHg)	LVEDP (mmHg)	LVDP (mmHg)	+dP/dt (mmHg/s)	−dP/dt (mmHg/s)	Heart rate (bpm)	RPP[A]
Wild type							
Control (n = 8)	98 ± 4	10.7 ± 0.2	87 ± 4	3,560 ± 160	2,790 ± 180	460 ± 14	450 ± 26
DEX (n = 5)	97 ± 4	10.4 ± 0.2	86 ± 5	3,590 ± 190	3,110 ± 120	442 ± 23	429 ± 32
DEX+NS398 (n = 6)	97 ± 4	10.8 ± 0.3	87 ± 4	3,710 ± 200	3,260 ± 210	462 ± 14	449 ± 21
NS398 (n = 5)	96 ± 4	10.5 ± 0.3	85 ± 4	3,550 ± 220	3,140 ± 180	445 ± 25	430 ± 34
RU486+DEX (n = 6)	99 ± 2	10.2 ± 0.4	89 ± 2	3,530 ± 110	3,090 ± 110	450 ± 16	448 ± 24
RU486 (n = 5)	98 ± 2	10.6 ± 0.5	87 ± 2	3,520 ± 210	2,700 ± 280	425 ± 13	421 ± 27
L-PGDS knockout							
Control (n = 8)	100 ± 4	10.5 ± 0.4	90 ± 4	3,690 ± 210	2,900 ± 180	463 ± 20	435 ± 11
DEX (n = 8)	100 ± 4	10.5 ± 0.2	90 ± 4	3,560 ± 100	2,860 ± 80	446 ± 25	444 ± 26

LVSP, LV systolic pressure; RPP, rate-pressure product. [A]Values denote mmHg × bpm (×100).

preting data obtained from lipodomics using a single remotely related internal standard. Estimates of the quantitative changes in prostaglandin formation must be viewed as preliminary, given the absence of authentic internal standards. We estimated based on the capacity to generate prostanoids in serum and cardiac tissue rather than on actual rates of biosynthesis. Additionally, we isolated adult mouse cardiomyocytes and stimulated them with corticosteroids. As shown in Figure 3E, COR and CVZ, but not ALD, increased the expression levels of *Pla2g4a*, *Ptgs2*, and *Ptgds* in cultured adult mouse cardiomyocytes.

Glucocorticoid pretreatment attenuates myocardial ischemia/reperfusion injury in a COX2-dependent manner in isolated perfused hearts. The effect of glucocorticoid-GR signaling on functionality during ischemia/reperfusion injury was studied in Langendorff-perfused mice hearts. Mice were injected i.p. with 2 mg/kg DEX, and 24 hours later, the hearts were isolated and subjected to 30 minutes of total global ischemia followed by 60 minutes of aerobic reperfusion. DEX pretreatment did not affect the cardiac parameters at baseline (Table 1), whereas it significantly improved recovery of LV developed pressure (LVDP), as well as positive and negative LV peak *dP/dt* (+*dP/dt* and -*dP/dt*, respectively), during reperfusion ($P < 0.05$ versus control; Figure 4, A–E). Consistent with these findings, DEX significantly attenuated total LDH release into the perfusate during reperfusion compared with the control ($P < 0.05$; Figure 4F). In mice injected i.p. with 20 mg/kg RU486 1 hour before DEX injection, the augmentation of functional recovery and the reduction in total LDH release after ischemia/reperfusion were abrogated. These results strongly suggest that the cardioprotective effects of DEX are mediated through the GR. RU486 alone altered neither cardiac parameters at baseline (Table 1) nor functional recovery after ischemia/reperfusion (data not shown).

To investigate the possibility that COX2 acts as a downstream effector of DEX-GR–mediated signaling, mice were injected i.p. with 5 mg/kg NS398, a selective COX2 inhibitor, 40 minutes prior to excision of the heart. There was no difference in LV function before the induction of ischemia between the DEX alone and DEX plus NS398 groups (Table 1). Notably, NS398 completely suppressed both the improvement of LV functional recovery and the reduction in LDH release into the perfusate conferred by DEX treatment (Figure 5, A–F). As previously reported, NS398 alone does not exacerbate the degree of ischemia/reperfusion injury (19, 20).

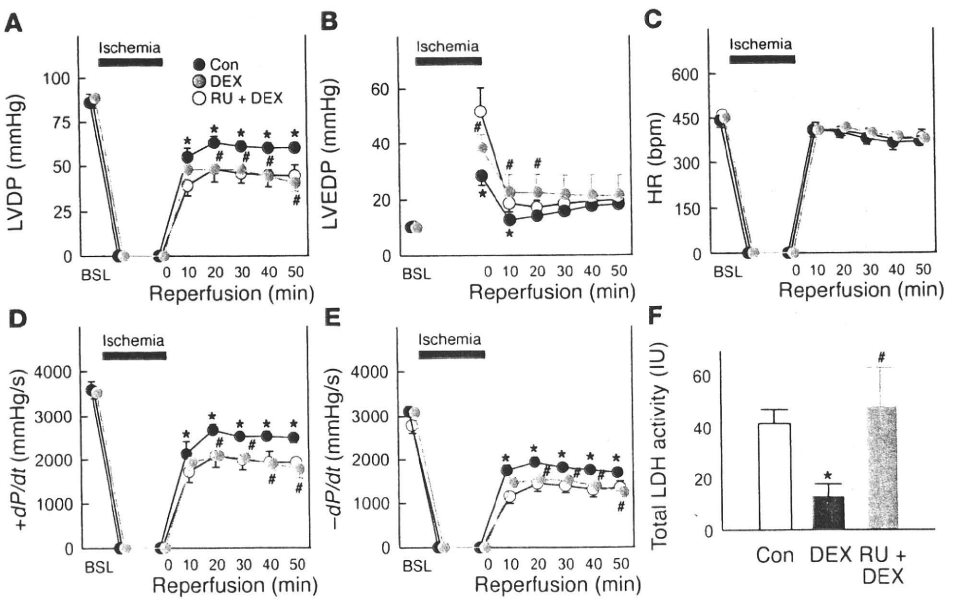

Figure 4
Glucocorticoid protects the heart against ischemia/reperfusion injury acting via the GR. Mice were injected i.p. with either 2 mg/kg DEX (n = 5) or vehicle control (n = 8). At 1 hour before the DEX injection, a group of mice was injected i.p. with 20 mg/kg RU486 (RU + DEX; n = 6). At 24 hours after DEX injection, hearts were isolated and subjected to 30 minutes of total global ischemia followed by aerobic reperfusion. BSL, baseline. (**A**) Recovery of LVDP. (**B**) LVEDP. (**C**) Recovery of heart rate. (**D**) Recovery of +*dP/dt*. (**E**) Recovery of −*dP/dt*. (**F**) LDH release in the perfusate. *$P < 0.05$ versus vehicle; #$P < 0.05$ versus DEX; ANOVA.

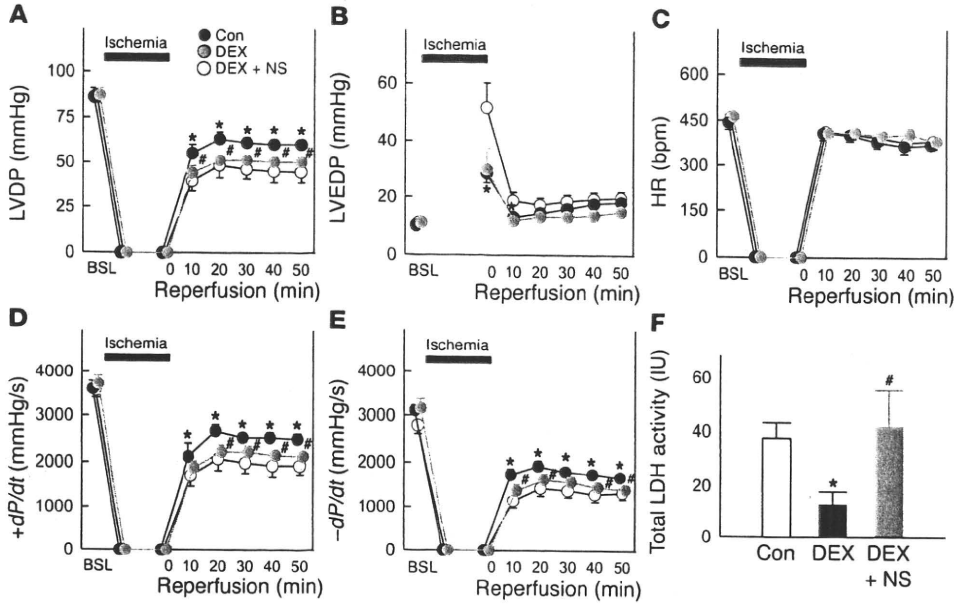

Figure 5
A COX2 inhibitor completely blocks the cardioprotective effect of glucocorticoid against ischemia/reperfusion injury. Mice were injected i.p. with the selective COX2 inhibitor NS398 (NS) at 5 mg/kg 40 minutes prior to excision of the heart (n = 6). (**A**) Recovery of LVDP. (**B**) LVEDP. (**C**) Recovery of heart rate. (**D**) Recovery of $+dP/dt$. (**E**) Recovery of $-dP/dt$. (**F**) LDH release in the perfusate. $^{*}P < 0.05$ versus vehicle; $^{\#}P < 0.05$ versus DEX; ANOVA.

Genetic deletion of L-PGDS abrogates the cardioprotective effect afforded by glucocorticoids to isolated perfused hearts. To examine the role of L-PGDS-catalyzed PGD_2 biosynthesis in the cardioprotective effect of glucocorticoid-GR signaling, L-PGDS-knockout mice were injected i.p. with either 2 mg/kg DEX or vehicle; 24 hours later, the hearts were isolated and subjected to 30 minutes of total global ischemia followed by 60 minutes of aerobic reperfusion. There was no difference in LV function before the induction of ischemia between the hearts from the L-PGDS-knockout mice and those from the wild-type control mice (Table 1). As expected, the expression levels of L-PGDS were negligible in the DEX-treated and vehicle-treated L-PGDS-knockout mouse hearts (Figure 6A). DEX did not improve the recovery of LVDP, $+dP/dt$, or $-dP/dt$ and did not reduce total LDH release into the perfusate during reperfusion of L-PGDS-knockout hearts (n = 8 per group; Figure 6, B–G).

Glucocorticoids reduce infarct size in an L-PGDS–dependent manner after ischemia/reperfusion injury in vivo. We subjected hearts to myocardial ischemia/reperfusion injury in vivo. Initially, we examined whether the level of PGD_2 was increased in the ischemic myocardium in the absence of DEX pretreatment by quantifying the levels

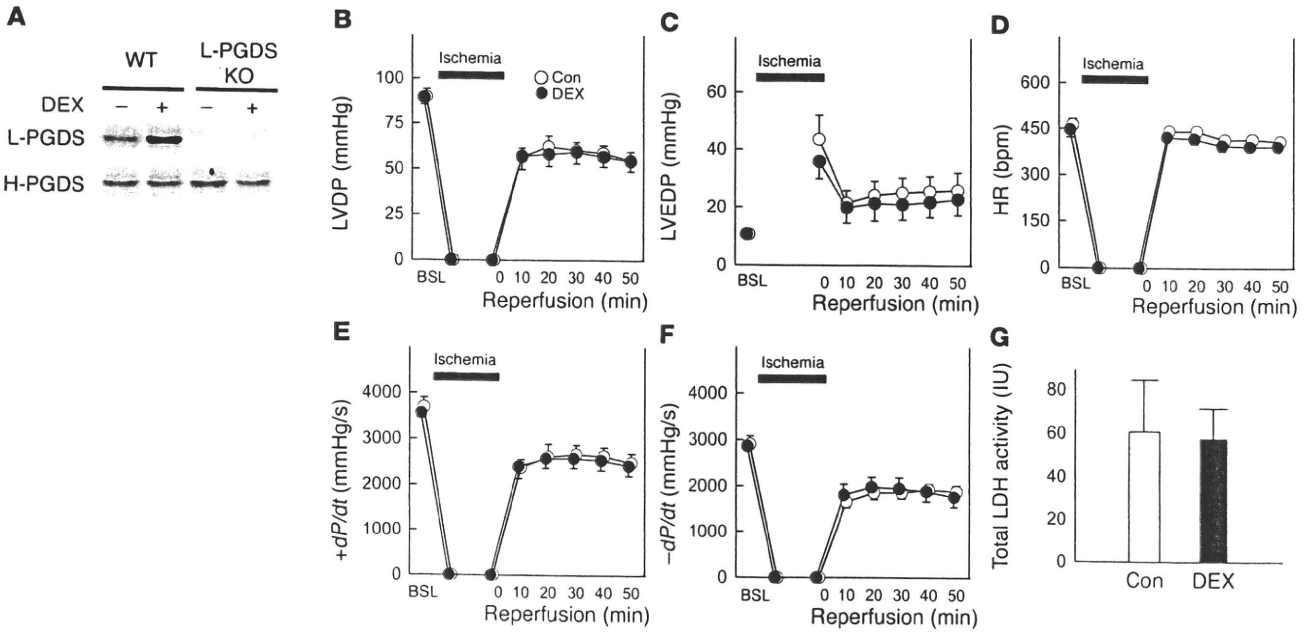

Figure 6
Lack of cardioprotective effect of glucocorticoid in L-PGDS–knockout mice. L-PGDS–knockout mice were injected i.p. with either 2 mg/kg DEX (n = 8) or vehicle control (n = 8). (**A**) Protein levels of L-PGDS and H-PGDS were determined by Western blotting. (**B**) Recovery of LVDP. (**C**) LVEDP. (**D**) Recovery of heart rate. (**E**) Recovery of $+dP/dt$. (**F**) Recovery of $-dP/dt$. (**G**) LDH release in the perfusate.

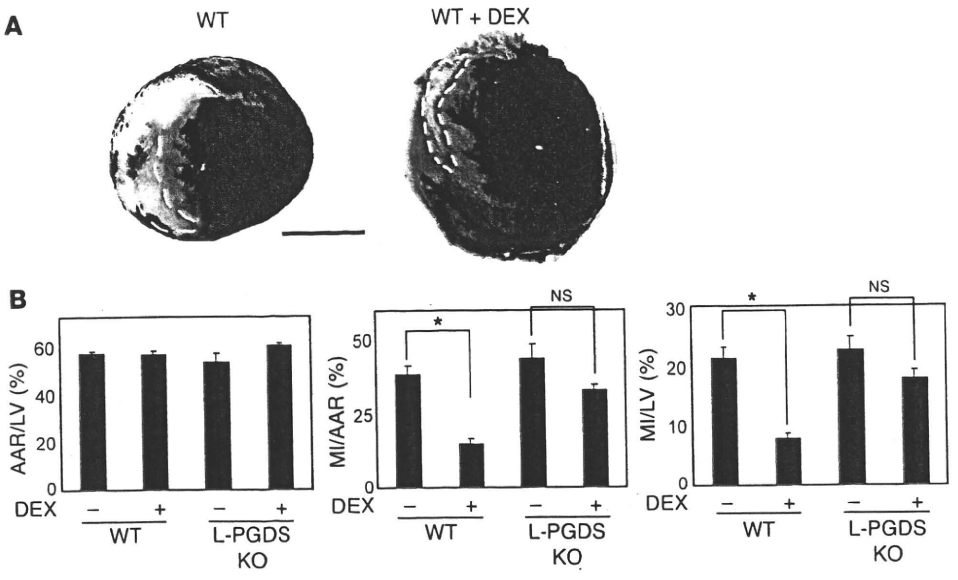

Figure 7
Reproduction of the L-PGDS–dependent cardioprotective effect of DEX in in vivo ischemia/reperfusion. (**A**) Representative photographs of heart sections obtained from wild-type mice subjected to myocardial ischemia/reperfusion injury in the presence or absence of DEX pretreatment. Areas of infarct are denoted by dotted white outlines. Scale bar: 4 mm. (**B**) Effect of DEX pretreatment on infarct size, expressed as a ratio of area at risk (AAR) to LV, of total infarct area (MI) to area at risk, and of total infarct area to LV ($n = 5$). $^*P < 0.05$.

of the 3 major prostanoids in the hearts 10 minutes after reoxygenation. Ischemia itself had no effect on the intramyocardial levels of PGD_2 (Supplemental Figure 2).

We then investigated whether DEX could protect the in vivo heart against ischemia/reperfusion injury. Pretreatment with DEX did not affect the plasma levels of PGD_2, but significantly attenuated the levels of plasma PGE_2 compared with the untreated mice ($P < 0.0001$; $n = 7$; Supplemental Figure 3). Immunohistologic analyses revealed that L-PGDS was predominantly expressed in the myocardium at the infarct border zone, but not in the infiltrating cells after reperfusion (Supplemental Figure 4). DEX had no effects on the expression levels of the D-type prostanoid (DP) receptor and the chemoattractant receptor-like molecule expressed on Th2 cells (CRTH2; also known as DP2) in the heart (Supplemental Figure 1). Consistent with the results of the ex vivo analysis using isolated Langendorff-perfused hearts, pretreatment with DEX significantly reduced the ratio of infarct size to area at risk after ischemia/reperfusion in the wild-type mice (Figure 7A). We also performed myocardial ischemia/reperfusion in L-PGDS–knockout mice. The infarct sizes for the L-PGDS–knockout and wild-type mice without DEX pretreatment were similar. Interestingly, the cardioprotective effect of DEX was markedly reduced in L-PGDS–knockout mice compared with wild-type mice (Figure 7B).

Glucocorticoid-GR signaling protects cultured cardiomyocytes from anoxia/reoxygenation injury via COX2- and L-PGDS–dependent PGD_2 synthesis. To examine more directly the effects of glucocorticoids on cardiomyocyte viability, cultured cardiomyocytes were exposed to glucose-free hypoxia followed by reoxygenation. CVZ suppressed cell death caused by glucose-free hypoxia and reoxygenation, and this effect was abrogated by siRNA-mediated knockdown of the GR or pretreatment with RU486 (Figure 8, A–D), which suggests that CVZ-mediated survival signaling is regulated through the GR. To examine the possibility that COX2 acts as a downstream effector of the GR-mediated survival pathway, we investigated the impact of COX2 inhibition on CVZ-mediated protection against cell death. Inhibition of COX2 activity by siRNA-mediated knockdown of *Ptgs2* or treatment with 10 μM NS398 blocked the cytoprotective effect of CVZ under the conditions of glucose-free hypoxia and reoxygenation (Figure 8, A–D). In addition, siRNA-mediated knockdown of *Ptgds* abrogated the cytoprotective effect of CVZ against glucose-free hypoxia and reoxygenation. This indicates that PGD_2 production via the COX2/L-PGDS–mediated pathway plays a crucial role in the cardioprotective effect of CVZ.

To examine the direct effect of PGD_2 on cardiomyocytes, these cells were stimulated with 30 nM PGD_2, and the activated signaling cascades were evaluated. Among the MAPKs, PGD_2 selectively activated ERK in cultured cardiomyocytes (Figure 9A). Activation of ERK occurred within 5 minutes and continued for as long as 120 minutes after PGD_2 stimulation. PGD_2 activated ERK in a dose-dependent manner (Figure 9B). The DP receptor antagonist BWA868C (10 μM) significantly attenuated PGD_2-induced ERK activation, while the CRTH2 receptor antagonist CAY10471 (10 μM) did not (Figure 9C). PGD_2 (30 nM) protected the cardiomyocytes against cell death caused by glucose-free hypoxia and reoxygenation. Pharmacologic and genetic disruption of the DP receptor, but not of the CRTH2 receptor, significantly abrogated the cardioprotective effect of PGD_2 under the conditions of glucose-free hypoxia and reoxygenation (Figure 10, A–D, and Supplemental Figure 5). The MEK inhibitor PD98059 (20 μM) also significantly abrogated the cardioprotective effect of PGD_2.

Discussion

In the present study, we demonstrated that glucocorticoids stimulated the common pathway for prostaglandin biosynthesis through the upregulation of cPLA2-COX2 expression via the GR in cardiomyocytes. The concordant induction of L-PGDS by glucocorticoids resulted in the activation of PGD_2 biosynthesis. We found that PGD_2-dominated activation of prostanoid biosynthesis accounted for the cardioprotective effects of glucocorticoids against ischemia/reperfusion injury. PGD_2 exerted its cardioprotective effects through the DP receptor on cardiomyocytes. Moreover, ERK1/2 was the major downstream kinase involved in PGD_2-DP–mediated cardioprotection.

Unexpectedly, we found that glucocorticoids induced the expression of mRNA for 2 key enzymes in prostaglandin synthesis, cPLA2 and COX2. These results indicate that glucocorticoid-GR signaling stimulates the common pathway for prostaglandin synthesis,

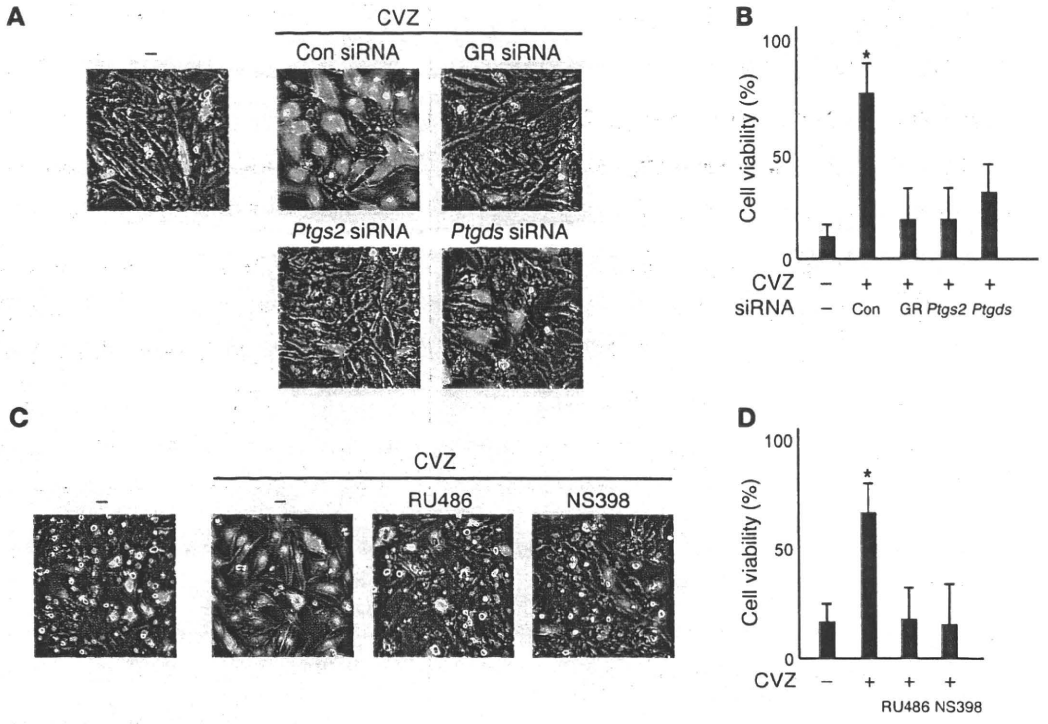

Figure 8

Glucocorticoid protects against cardiomyocyte death induced by anoxia/reoxygenation injury in GR-, COX2-, and L-PGDS–dependent manners. (**A** and **C**) Neonatal rat cardiomyocytes were (**A**) transfected with control-, GR-, *Ptgs2*-, and *Ptgds*-specific siRNAs or (**B**) pretreated with 10 μM RU486 or NS398. The cells were subjected to glucose-free anoxia for 5 hours, followed by reoxygenation. Dead cells (red nuclei) and viable cells (green) were quantified as described in Methods. Scale bars: 100 μm. (**B** and **D**) Viable cells from the experiments shown in **A** and **C**, respectively, were quantified by counting 100 cells in 5 independent experiments ($n = 5$). *$P < 0.05$ versus vehicle; Student's t test.

which begins with the liberation of arachidonic acids and ends with the synthesis of PGH_2. In inflammatory cells, such as monocytes/macrophages, fibroblasts, and endothelial cells, the GR blocks the expression of cPLA2 and COX2, thereby inhibiting prostaglandin synthesis (10–12). The molecular mechanism underlying the inhibitory effect of the GR on signal-dependent induction of *Pla2g4a* and *Ptgs2* transcription has been studied intensively as a prototypic example of transrepression by the GR (10–12). In contrast, in the present study, we found that glucocorticoid increased rather than suppressed the expression level of *Ptgs2* mRNA, even in the presence of IL-1β–mediated signaling, in cardiomyocytes.

In amniotic cells, the GR upregulates the expression of *Pla2g4a* and *Ptgs2*, as seen in cardiomyocytes (21–23). Interestingly, the glucocorticoid concentrations in the maternal and fetal circulations, as well as those in the amniotic fluid, increase toward the end of gestation and at the onset of labor. As PGE_2 production by the amnion is involved in the onset and progression of labor, these paradoxical stimulatory effects of glucocorticoids on prostanoid biosynthesis are believed to affect the feed-forward loops that trigger parturition. The upregulation of *Ptgs2* mRNA expression has been detected after myocardial infarction (24), as well as in the failing human heart (25), concomitant with increases in the circulating cortisol levels (26). There may be a causal relationship between increased circulatory levels of glucocorticoids and the induction of COX2.

The relative abundance of a specific prostanoid is determined by the expression and activity of its specific isomerase. Of the PGH_2 isomerases, we found that glucocorticoids selectively increased the expression level of L-PGDS via the GR in cardiomyocytes. Accumulating evidence suggests that L-PGDS–mediated, PGD_2-dominated eicosanoid production exerts protective effects on the vascular system. L-PGDS is expressed in the endothelial cells and in the synthetic state of smooth muscle cells in the atherosclerotic plaque (27). COX2 expression, when accompanied by minimal PGE_2 synthesis and high PGD_2 levels, may contribute to the resolution of inflammation (28). PGD_2 prevents platelet aggregation (29) and induces endothelial-dependent arterial relaxation (30). Furthermore, the PGD_2 metabolite J series of prostanoids, such as 15-deoxy-$\Delta^{12,14}$-PGJ_2, exerts several antiinflammatory and antioxidant effects through a mechanism that involves the activation of PPARγ (31). Indeed, L-PGDS–knockout mice are prone to develop atherosclerosis when fed a high-fat diet (32). Furthermore, atherosclerotic plaque instability appears to be determined by the balance between L-PGDS–mediated PGD_2 synthesis and mPGES-1–mediated PGE_2 synthesis (33). It is of clinical interest that an increase in serum L-PGDS levels 48 hours after PTCA correlates with the avoidance of restenosis (34). Similarly, renal protective effects of L-PGDS–mediated PGD_2 biosynthesis have been proposed. Urinary L-PGDS excretion markedly increases during the early stage of kidney injury, as in diabetic nephropathy (35). PGD_2 inhibits the TGF-β1–induced epithelial-to-mesenchymal transition in cultured renal epithelial cells (36). A renal protective role for L-PGDS is supported by the recent genetic evidence that L-PGDS–knockout mice develop glomerular hypertrophy, tubular damage, and renal fibrosis (32).

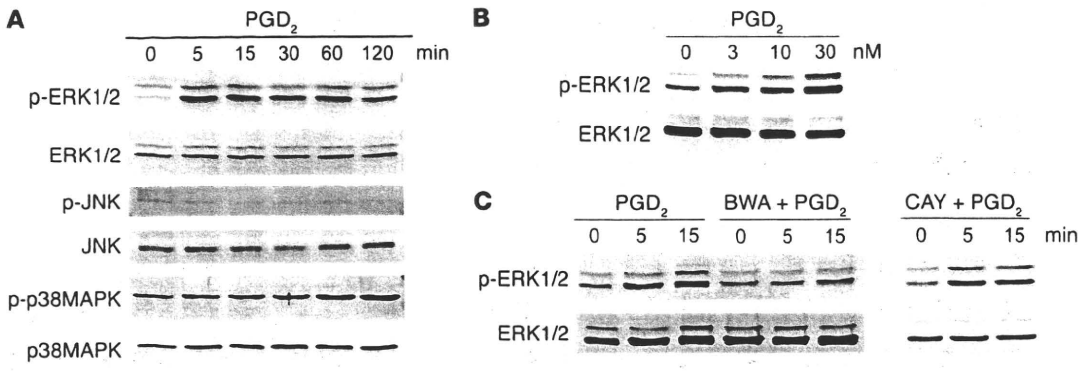

Figure 9

PGD_2 activates ERK1/2 via the DP receptor in cultured cardiomyocytes. (**A**) Neonatal rat cardiomyocytes were stimulated with 30 nM PGD_2 for the indicated times. Activation of MAPKs was detected by Western blotting using the respective antibodies directed against the phosphorylated forms of ERK1/2, JNK, and p38MAPK. The membranes were then stripped and reprobed with antibodies against ERK1/2, JNK, and p38MAPK. (**B**) Cells were stimulated with the indicated concentrations of PGD_2, and the activation of ERK1/2 was determined by Western blotting. (**C**) Cells were pretreated with 10 μM BWA868C (BWA) or 10 μM CAY10471 (CAY) and stimulated with 30 nM PGD_2. Lanes for combined CAY10471 and PGD_2 treatment were run on a separate gel.

L-PGDS is also highly expressed in the heart, being localized primarily to the atrial and ventricular cardiomyocytes, and levels of L-PGDS are elevated in the coronary circulation of patients with severe coronary heart disease (27). However, the factors that control *Ptgds* gene expression and the physiologic and pathophysiologic roles of L-PGDS in cardiomyocytes are poorly understood. The present study is, to the best of our knowledge, the first to demonstrate that glucocorticoids preferentially promote PGD_2 biosynthesis in cardiomyocytes through concomitant induction of L-PGDS and the cPLA2-COX2 pathway via the GR. Coordinated stimulation of the cPLA2-COX2-L-PGDS pathway is crucial for glucocorticoid-induced cardioprotection in the setting of ischemia/reperfusion injury, since glucocorticoid-enhanced recovery of LV function after ischemia/reperfusion was completely abrogated by either pharmacologic inhibition of COX2 or genomic disruption of L-PGDS. Furthermore, these results suggest that the function of L-PGDS as a PGD_2-producing enzyme is more important than its function as a transporter of lipophilic ligands, at least in the setting of glucocorticoid-induced cardioprotection against ischemia/reperfusion injury.

There were no changes with respect to the functional recovery of ex vivo hearts or the infarct sizes of the in vivo hearts after ischemia/reperfusion in the L-PGDS–knockout mice compared with wild-type mice without DEX pretreatment. However, these results do not exclude the potential cardioprotective effects of L-PGDS–derived PGD_2 production via the GR in response to physiologic elevations of the glucocorticoid levels after myocardial infarction. The activation of L-PGDS-mediated PGD_2 biosynthesis may mitigate pathologic ventricular remodeling in the late phase of acute myocardial infarction.

The cytoprotective effects of glucocorticoids that occur via the activation of PGD_2-dominated eicosanoid synthesis in cardiomyocytes were reproduced in an in vitro culture system. Glucocorticoid-GR signaling protected against cell death induced by glucose-free anoxia and reoxygenation of cultured cardiomyocytes. This cardioprotective action of glucocorticoids was abrogated by knockdown of either COX2 or L-PGDS. Conversely, PGD_2 itself protected cardiomyocytes against death caused by glucose-free anoxia and reoxygenation. These findings suggest that the PGD_2 produced by glucocorticoids in cardiomyocytes acts as a local mediator in both autocrine and paracrine fashions.

The DP receptor and the CRTH2 receptor, 2 distinct G protein–coupled receptors, have been identified as PGD_2 receptors. We found that the cardioprotective effects of PGD_2 in culture were chiefly mediated through the DP receptor. PGD_2 also mediates neuronal protection against ischemia/reperfusion injury via the DP receptor (37). With respect to signaling downstream of the DP receptor, we demonstrated that ERK1/2 was the major pathway for PGD_2–DP receptor–mediated protection of cardiomyocytes. Notably, ERK1/2 has been regarded as an integral part of the reperfusion injury salvage kinase that confers cardioprotection (38). However, PGD_2 is a relatively unstable product that is readily metabolized to the more stable J series of prostanoids. Further studies using distinct PGD_2 receptor–knockout mice are necessary to elucidate the receptor-dependent and/or -independent mechanisms underlying the cardioprotection afforded by PGD_2 to hearts in vivo.

The clinical significance of glucocorticoid administration remains controversial. The ambiguity of glucocorticoid effectiveness may be ascribed to the inappropriate design of clinical studies based on incomplete understanding of the fundamental mechanism of glucocorticoid action in the heart. The activities of glucocorticoids are diverse and are altered in time- and space-dependent manners. Furthermore, functional redundancy exists between GR and MR at the level of ligand-binding specificity, and the heart expresses both the GR and the MR. Therefore, we attempted to elucidate the heart-specific functions of glucocorticoid-GR signaling independently of the functional redundancy with MR. Our results indicated that glucocorticoids directly induced *Pla2g4a*, *Ptgs2*, and *Ptgds* expression via the GR in cardiomyocytes, and that the subsequent increase in PGD_2 protected cardiomyocytes against cell death induced by ischemia/reperfusion in both autocrine and paracrine manners. Considering the functional overlap between the GR and the MR at the level of ligand binding specificity, the cardioprotective effects of glucocorticoids may be offset by proinflammatory MR activation in response to stress, which includes acute myocardial infarction (14). In terms of overcoming this lim-

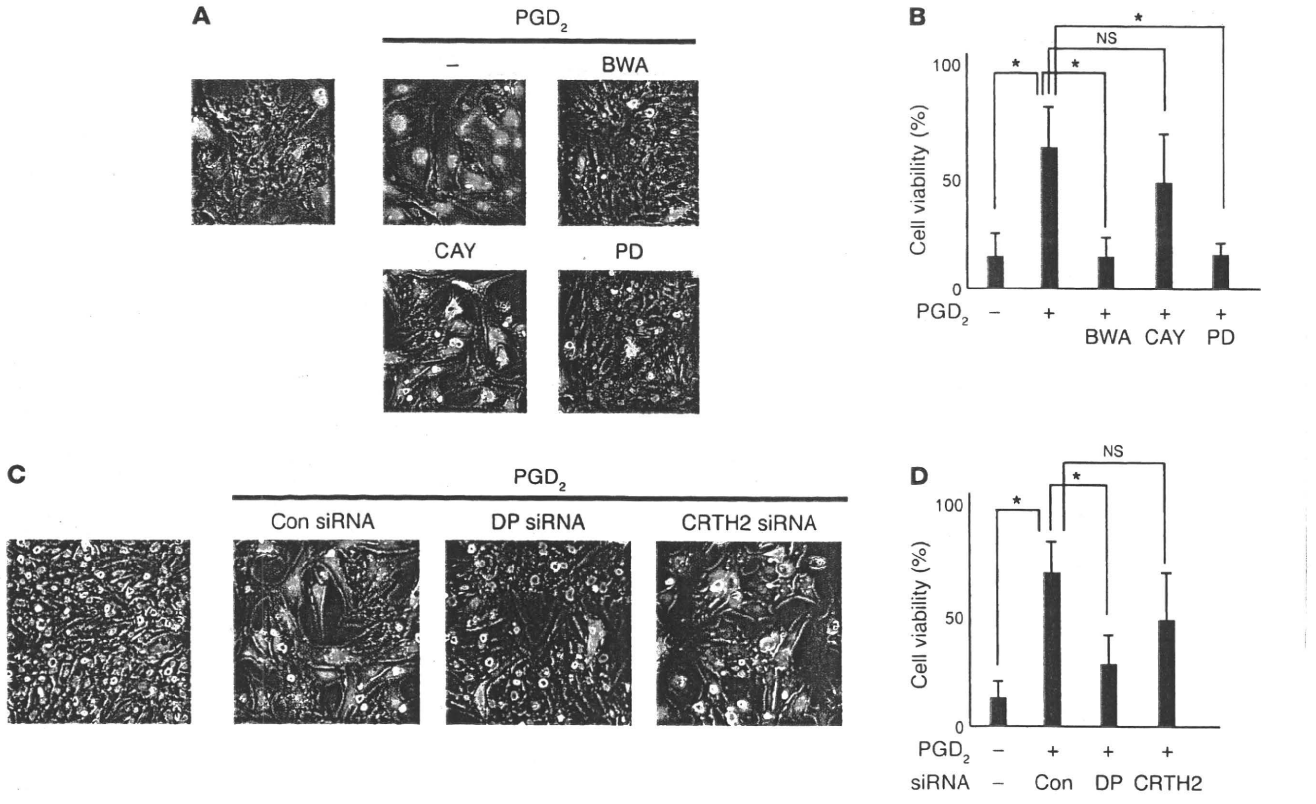

Figure 10

PGD_2 protects against cardiomyocyte death induced by anoxia/reoxygenation injury via the DP receptor and ERK1/2 signaling. (**A** and **B**) Neonatal rat cardiomyocytes were stimulated with 30 nM PGD_2 in the presence or absence of 10 μM BWA868C, 10 μM CAY10471, or 20 μM PD98059 (PD) and then subjected to glucose-free anoxia followed by reoxygenation. (**A**) Dead cells (red nuclei) and viable cells (green) were determined as described in Methods. Scale bars: 100 μm. (**B**) Viable cells were quantified by counting 100 cells in 5 independent experiments ($n = 5$). (**C** and **D**) Neonatal rat cardiomyocytes were transfected with control-, DP-, or CRTH2-specific siRNA. Reductions in the expression levels of the target genes were confirmed by Q-PCR (see Supplemental Figure 5). Cells were treated with 30 nM PGD_2 and then subjected to glucose-free anoxia followed by reoxygenation. (**C**) Dead cells (red nuclei) and viable cells (green) were determined as described in Methods. Scale bars: 100 μm. (**D**) Viable cells were quantified by counting 100 cells in 5 independent experiments ($n = 5$). $^*P < 0.05$; Student's t test.

itation, GR-selective agonists, such as DEX and betamethasone, may have clinical advantages over nonselective GR agonists (e.g., prednisolone and cortisol) in limiting infarct size and improving mortality after myocardial infarction.

Methods

Animals. All animal experiments were reviewed and approved by the Institutional Animal Care and Use Committee at the Keio University School of Medicine. L-PGDS–knockout mice were generated as previously described (39).

Gene expression. Neonatal ventricular myocytes from 1- to 2-day-old Sprague-Dawley rats were subjected to Percoll gradient centrifugation and differential plating in order to enrich for cardiac myocytes and deplete nonmyocyte populations (40). Total RNA was isolated and hybridized to the GeneChip Rat Genome 230 2.0 Array (Affymetrix), composed of 31,042 probe sets representing approximately 28,000 rat genes. Q-PCR was performed using the ABI Prism 7700 sequence detection system (Applied Biosystems). Predesigned gene-specific primer and probe sets (TaqMan Gene Expression Assays) were used. The 18s ribosomal RNA was amplified as an internal control.

Western blotting. Nuclear extracts were prepared as previously described (41). Rabbit polyclonal antibodies against GR and goat polyclonal antibodies against COX2 were purchased from Santa Cruz Biotechnology. Rabbit polyclonal antibodies directed against COX-1 were purchased from Alexis, and rabbit polyclonal antibodies directed against L-PGDS, mPGES1, mPGES2, cytosolic PGE synthase, DP, and CRTH2 were purchased from Cayman Chemical. Protein expression was visualized using horseradish peroxidase–conjugated secondary antibodies and enhanced chemiluminescence (Amersham Biosciences) and was detected using the LAS-3000 luminoimage analyzer (Fujifilm).

ELISA. Neonatal rat cardiomyocytes were treated with 100 nM CVZ for 24 hours. The levels of PGD_2, PGE_2, and 6-keto-$PGF_{1\alpha}$ in the culture media were measured using a commercial ELISA kit (Cayman Chemical) according to the manufacturer's instructions.

Oxidized phospholipid analysis by LC-MS/MS. The frozen hearts were homogenized in methanol that contained 2 internal standards (LTB4-d4 and 17:0-LPC), and oxidative fatty acids and oxidative phospholipids were extracted using solid-phase extraction. LC-MS/MS analysis was performed using the 4000 Q-TRAP quadrupole linear ion-trap hybrid mass spectrometer (Applied Biosystems/MDS Sciex) with the ACQUITY Ultra Performance LC (Waters). Specific detection was performed by multiple reaction monitoring (18).

Glucose-free hypoxia and reoxygenation. An anaerobic jar that contained an Anaero Pack (Mitsubishi Gas Chemical) was used to expose the cells to hypoxic stress (42). The medium used to grow the cardiomyocytes was replaced with glucose-free DMEM before the cells were exposed to hypoxic stress. After 5 hours of exposure of hypoxia, the medium was replaced

with 10% FBS-containing DMEM (reoxygenation medium). Cell viability was determined by the LIVE/DEAD Viability/Cytotoxicity Assay Kit (Invitrogen) based on the simultaneous determination of live and dead cells with the calcein AM and ethidium homodimer-1 probes, which are specific for intracellular esterase activity and membrane integrity, respectively. Fluorescence imaging of the cells was performed with a fluorescence microscope (BZ-9000; Keyence): live cells were labeled green, whereas the nuclei of dead cells were labeled red.

siRNA oligonucleotides and transfection. siRNA oligonucleotides against the rat *GR*, *Ptgs2*, and *Ptgds* genes, as well as control siRNA, were purchased from Ambion. Transfection of these siRNA oligonucleotides was performed using the Lipofectamine RNAiMAX Reagent (Invitrogen).

Langendorff perfusion of the heart. Hearts were excised rapidly from heparinized mice, perfused with modified Krebs-Henseleit buffer (120 mmol/l NaCl, 25 mmol/l $NaHCO_3$, 5.9 mmol/l KCl, 1.2 mmol/l $MgSO_4$, 1.75 mmol/l $CaCl_2$, and 10 mmol/l glucose), and gassed with 95% O_2 and 5% CO_2 at 37°C according to the Langendorff procedure. Coronary perfusion pressure was maintained at 90 mmHg. A plastic catheter with a polyethylene balloon was inserted into the LV through the left atrium. Before the induction of ischemia, the LV end-diastolic pressure (LVEDP) was adjusted to 10 mmHg by filling the balloon with water. Indices of LV function (LV systolic pressure; LVEDP; LVDP, calculated as the difference between LVSP and LVEDP; $+dP/dt$; and $-dP/dt$) were recorded as described previously (43). Rate-pressure product was calculated as the product of LV systolic pressure and heart rate. Total LDH activity released into the perfusate was measured with a commercially available kit (Sigma-Aldrich).

In vivo myocardial ischemia/reperfusion model. Regional myocardial ischemia was induced by transient occlusion of the left anterior descending coronary artery. After 30 minutes of ischemia, the tube used for myocardial reperfusion we removed, and the thorax was closed with the suture intact. The suture around the coronary artery was retied 2 hours after reperfusion, and 2% Evans blue dye was injected into the LV cavity to delineate retrospectively the area at risk for myocardial infarction. The heart was removed, washed in PBS, and then sliced into sequential 1-mm-thick sections. The sections were stained with 2,3,5-triphenyltetrazolium chloride (TTC; 3%), and the infarct (white), noninfarct (red), nonischemic (blue), and at-risk areas (white and red) were measured.

Immunohistochemistry. Hearts were perfused from the apex with PBS, perfusion fixed with 4% paraformaldehyde in PBS, dissected, subsequently cryoprotected in sucrose solution at 4°C, embedded in OCT compound (Miles Scientific), and snap-frozen in liquid nitrogen. The fixed hearts were sectioned (8-μm thickness) using the CM3050S cryostat (Leica). For immunostaining, the sections were blocked in 5% BSA for 30 minutes at room temperature and then treated with anti-L-PGDS and anti-CD45 antibodies (BD Biosciences — Pharmingen) overnight at 4°C. Secondary antibodies conjugated to Alexa Fluor 546 or Alexa Fluor 488 (Invitrogen) were applied at 1:200 dilutions for 1 hour at 4°C. Nuclei were stained with TOTO-3 (Invitrogen) in a mounting medium. The slides were observed under a fluorescence microscope (Olympus BX-60).

Statistics. Values are presented as mean ± SEM. Statistical significance was evaluated using 2-tailed, unpaired Student's *t* tests for comparisons of 2 mean values. Multiple comparisons involving more than 3 groups were performed using ANOVA. A *P* value less than 0.05 was considered statistically significant.

Acknowledgments

We thank M. Nishijima, M. Murakami, and M. Arita for critical discussion and M. Abe, K. Miyake, K. Kaneki, Y. Shiozawa, and T. Maruyama for technical assistance. M. Sano is a core member of the Global Center of Excellence (GCOE) for Human Metabolomics Systems Biology at MEXT. This work was supported by a PRESTO (Metabolism and Cellular Function) grant from the Japanese Science and Technology Agency (to M. Sano) and by the Vehicle Racing Commemorative Foundation (to M. Sano and K. Shinmura).

Received for publication September 10, 2008, and accepted in revised form March 18, 2009.

Address correspondence to: Motoaki Sano, Department of Regenerative Medicine and Advanced Cardiac Therapeutics, Keio University School of Medicine, 35 Shinanomachi Shinjuku-ku, Tokyo 160-8582, Japan. Phone: 81-3-5363-3874; Fax: 81-3-5363-3875; E-mail: msano@sc.itc.keio.ac.jp.

1. Sapolsky, R.M., Romero, L.M., and Munck, A.U. 2000. How do glucocorticoids influence stress responses? Integrating permissive, suppressive, stimulatory, and preparative actions. *Endocr. Rev.* **21**:55–89.
2. Libby, P., Maroko, P.R., Bloor, C.M., Sobel, B.E., and Braunwald, E. 1973. Reduction of experimental myocardial infarct size by corticosteroid administration. *J. Clin. Invest.* **52**:599–607.
3. Valen, G., et al. 2000. Glucocorticoid pretreatment protects cardiac function and induces cardiac heat shock protein 72. *Am. J. Physiol. Heart Circ. Physiol.* **279**:H836–H843.
4. Varga, E., et al. 2004. Inhibition of ischemia/reperfusion-induced damage by dexamethasone in isolated working rat hearts: the role of cytochrome c release. *Life Sci.* **75**:2411–2423.
5. Skyschally, A., et al. 2004. Glucocorticoid treatment prevents progressive myocardial dysfunction resulting from experimental coronary microembolization. *Circulation.* **109**:2337–2342.
6. Giugliano, G.R., Giugliano, R.P., Gibson, C.M., and Kuntz, R.E. 2003. Meta-analysis of corticosteroid treatment in acute myocardial infarction. *Am. J. Cardiol.* **91**:1055–1059.
7. Cronstein, B.N., Kimmel, S.C., Levin, R.I., Martiniuk, F., and Weissmann, G. 1992. Corticosteroids are transcriptional regulators of acute inflammation. *Trans. Assoc. Am. Physicians.* **105**:25–35.
8. Radomski, M.W., Palmer, R.M., and Moncada, S. 1990. Glucocorticoids inhibit the expression of an inducible, but not the constitutive, nitric oxide synthase in vascular endothelial cells. *Proc. Natl. Acad. Sci. U. S. A.* **87**:10043–10047.
9. Hafezi-Moghadam, A., et al. 2002. Acute cardiovascular protective effects of corticosteroids are mediated by non-transcriptional activation of endothelial nitric oxide synthase. *Nat. Med.* **8**:473–479.
10. Pascual, G., and Glass, C.K. 2006. Nuclear receptors versus inflammation: mechanisms of transrepression. *Trends Endocrinol. Metab.* **17**:321–327.
11. Hayashi, R., Wada, H., Ito, K., and Adcock, I.M. 2004. Effects of glucocorticoids on gene transcription. *Eur. J. Pharmacol.* **500**:51–62.
12. De Bosscher, K., Vanden Berghe, W., and Haegeman, G. 2003. The interplay between the glucocorticoid receptor and nuclear factor-kappaB or activator protein-1: molecular mechanisms for gene repression. *Endocr. Rev.* **24**:488–522.
13. Walker, B.R. 2007. Glucocorticoids and cardiovascular disease. *Eur. J. Endocrinol.* **157**:545–559.
14. Funder, J.W. 2005. RALES, EPHESUS and redox. *J. Steroid Biochem. Mol. Biol.* **93**:121–125.
15. Yoshikawa, N., et al. 2002. Distinct interaction of cortivazol with the ligand binding domain confers glucocorticoid receptor specificity: cortivazol is a specific ligand for the glucocorticoid receptor. *J. Biol. Chem.* **277**:5529–5540.
16. Yoshikawa, N., et al. 2005. The distinct agonistic properties of the phenylpyrazolosteroid cortivazol reveal interdomain communication within the glucocorticoid receptor. *Mol. Endocrinol.* **19**:1110–1124.
17. Yoshikawa, N., et al. 2009. Ligand-based gene expression profiling reveals novel roles of glucocorticoid receptor in cardiac metabolism. *Am. J. Physiol. Endocrinol. Metab.* Online publication ahead of print. doi:10.1152/ajpendo.90767.2008.
18. Taguchi, R., Nishijima, M., and Shimizu, T. 2007. Basic analytical systems for lipidomics by mass spectrometry in Japan. *Methods Enzymol.* **432**:185–211.
19. Guo, Y., et al. 2000. Evidence for an essential role of cyclooxygenase-2 as a mediator of the late phase of ischemic preconditioning in mice. *Basic Res. Cardiol.* **95**:479–484.
20. Shibata, R., et al. 2005. Adiponectin protects against myocardial ischemia-reperfusion injury through AMPK- and COX-2-dependent mechanisms. *Nat. Med.* **11**:1096–1103.
21. Zakar, T., Hirst, J.J., Mijovic, J.E., and Olson, D.M. 1995. Glucocorticoids stimulate the expression of prostaglandin endoperoxide H synthase-2 in amnion cells. *Endocrinology.* **136**:1610–1619.
22. Economopoulos, P., Sun, M., Purgina, B., and Gibb, W. 1996. Glucocorticoids stimulate prostaglandin H synthase type-2 (PGHS-2) in the fibroblast cells

in human amnion cultures. *Mol. Cell. Endocrinol.* **117**:141–147.
23. Sun, K., et al. 2003. Glucocorticoids induce cytosolic phospholipase A2 and prostaglandin H synthase type 2 but not microsomal prostaglandin E synthase (PGES) and cytosolic PGES expression in cultured primary human amnion cells. *J. Clin. Endocrinol. Metab.* **88**:5564–5571.
24. Abbate, A., et al. 2004. Cyclo-oxygenase-2 (COX-2) expression at the site of recent myocardial infarction: friend or foe? *Heart.* **90**:440–443.
25. Wong, S.C., Fukuchi, M., Melnyk, P., Rodger, I., and Giaid, A. 1998. Induction of cyclooxygenase-2 and activation of nuclear factor-kappaB in myocardium of patients with congestive heart failure. *Circulation.* **98**:100–103.
26. Nito, I., Waspadji, S., Harun, S., and Markum, H.M. 2004. Correlation between cortisol levels and myocardial infarction mortality among intensive coronary care unit patients during first seven days in hospital. *Acta Med. Indones.* **36**:8–14.
27. Eguchi, Y., et al. 1997. Expression of lipocalin-type prostaglandin D synthase (beta-trace) in human heart and its accumulation in the coronary circulation of angina patients. *Proc. Natl. Acad. Sci. U. S. A.* **94**:14689–14694.
28. Gilroy, D.W., et al. 1999. Inducible cyclooxygenase may have anti-inflammatory properties. *Nat. Med.* **5**:698–701.
29. Bushfield, M., McNicol, A., and MacIntyre, D.E. 1985. Inhibition of platelet-activating-factor-induced human platelet activation by prostaglandin D2. Differential sensitivity of platelet transduction processes and functional responses to inhibition by cyclic AMP. *Biochem. J.* **232**:267–271.
30. Braun, M., and Schror, K. 1992. Prostaglandin D2 relaxes bovine coronary arteries by endothelium-dependent nitric oxide-mediated cGMP formation. *Circ. Res.* **71**:1305–1313.
31. Shibata, T., et al. 2002. 15-deoxy-delta 12,14-prostaglandin J2. A prostaglandin D2 metabolite generated during inflammatory processes. *J. Biol. Chem.* **277**:10459–10466.
32. Ragolia, L., et al. 2005. Accelerated glucose intolerance, nephropathy, and atherosclerosis in prostaglandin D2 synthase knock-out mice. *J. Biol. Chem.* **280**:29946–29955.
33. Cipollone, F., et al. 2004. Balance between PGD synthase and PGE synthase is a major determinant of atherosclerotic plaque instability in humans. *Arterioscler. Thromb. Vasc. Biol.* **24**:1259–1265.
34. Inoue, T., et al. 2001. Serum prostaglandin D synthase level after coronary angioplasty may predict occurrence of restenosis. *Thromb. Haemost.* **85**:165–170.
35. Uehara, Y. 2004. PGD(2)/L-PGDS system in hypertension and renal injury [In Japanese]. *Nippon Yakurigaku Zasshi.* **123**:23–33.
36. Zhang, A., Dong, Z., and Yang, T. 2006. Prostaglandin D2 inhibits TGF-beta1-induced epithelial-to-mesenchymal transition in MDCK cells. *Am. J. Physiol. Renal Physiol.* **291**:F1332–F1342.
37. Taniguchi, H., et al. 2007. Prostaglandin D2 protects neonatal mouse brain from hypoxic ischemic injury. *J. Neurosci.* **27**:4303–4312.
38. Yellon, D.M., and Hausenloy, D.J. 2007. Myocardial reperfusion injury. *N. Engl. J. Med.* **357**:1121–1135.
39. Eguchi, N., et al. 1999. Lack of tactile pain (allodynia) in lipocalin-type prostaglandin D synthase-deficient mice. *Proc. Natl. Acad. Sci. U. S. A.* **96**:726–730.
40. Sano, M., et al. 2002. Activation and function of cyclin T-Cdk9 (positive transcription elongation factor-b) in cardiac muscle-cell hypertrophy. *Nat. Med.* **8**:1310–1317.
41. Sano, M., et al. 2007. Intramolecular control of protein stability, subnuclear compartmentalization, and coactivator function of peroxisome proliferator-activated receptor gamma coactivator 1alpha. *J. Biol. Chem.* **282**:25970–25980.
42. Terai, K., et al. 2005. AMP-activated protein kinase protects cardiomyocytes against hypoxic injury through attenuation of endoplasmic reticulum stress. *Mol. Cell. Biol.* **25**:9554–9575.
43. Shinmura, K., et al. 2007. Cardioprotective effects of short-term caloric restriction are mediated by adiponectin via activation of AMP-activated protein kinase. *Circulation.* **116**:2809–2817.

Biochemical and Biophysical Research Communications 385 (2009) 497–502

Contents lists available at ScienceDirect

Biochemical and Biophysical Research Communications

journal homepage: www.elsevier.com/locate/ybbrc

In vitro pharmacologic testing using human induced pluripotent stem cell-derived cardiomyocytes

Tomofumi Tanaka [a,e,1], Shugo Tohyama [a,b,1], Mitsushige Murata [a], Fumimasa Nomura [c], Tomoyuki Kaneko [c], Hao Chen [a], Fumiyuki Hattori [a,e], Toru Egashira [a,b], Tomohisa Seki [a,b], Yohei Ohno [a,b], Uichi Koshimizu [e], Shinsuke Yuasa [a], Satoshi Ogawa [b], Shinya Yamanaka [d], Kenji Yasuda [c], Keiichi Fukuda [a,*]

[a] Department of Regenerative Medicine and Advanced Cardiac Therapeutics, School of Medicine, Keio University, Tokyo, Japan
[b] Cardiology Division, School of Medicine, Keio University, Tokyo, Japan
[c] Department of Biomedical Information, Institute of Biomaterials and Bioengineering, Tokyo Medical and Dental University, Tokyo, Japan
[d] Department of Stem Cell Biology, Institute for Frontier Medical Sciences, Kyoto University, Kyoto, Japan
[e] Biomedical Research Laboratories, Asubio Pharma Co., Ltd, Osaka, Japan

ARTICLE INFO

Article history:
Received 13 May 2009
Available online 21 May 2009

Keywords:
Arrhythmia
Human iPS cell
Cardiomyocyte
Drug screening
Ion channel

ABSTRACT

The lethal ventricular arrhythmia Torsade de pointes (TdP) is the most common reason for the withdrawal or restricted use of many cardiovascular and non-cardiovascular drugs. The lack of an *in vitro* model to detect pro-arrhythmic effects on human heart cells hinders the development of new drugs. We hypothesized that recently established human induced pluripotent stem (hiPS) cells could be used in an *in vitro* drug screening model. In this study, hiPS cells were driven to differentiate into functional cardiomyocytes, which expressed cardiac markers including Nkx2.5, GATA4, and atrial natriuretic peptide. The hiPS-derived cardiomyocytes (hiPS-CMs) were analyzed using a multi electrode assay. The application of ion channel inhibitors resulted in dose-dependent changes to the field potential waveform, and these changes were identical to those induced in the native cardiomyocytes. This study shows that hiPS-CMs represent a promising *in vitro* model for cardiac electrophysiologic studies and drug screening.

Torsade de pointes (TdP), which is a polymorphic ventricular tachycardia that can degenerate into ventricular fibrillation and subsequent cardiac sudden death, may be associated with drug-induced QT prolongation. Drug-induced TdP is a serious issue in drug development and safety, and has led to the withdrawal of many non-cardiovascular drugs. Despite the rarity of TdP in the clinical setting, definition of the pro-arrhythmic potential of a candidate drug is important in terms of patient safety and drug development. There is therefore an important need for a preclinical model to predict TdP. Several *in vivo* and *in vitro* models are currently used in cardiovascular drug development, testing, and screening for side-effects [1–3]. Inhibition of hERG, which is a rapid delayed rectifier current (I_{Kr}) that controls action potential (AP) repolarization, is the most common cause of QT prolongation induced by non-cardiac drugs. Thus, non-clinical evaluation of the potential for delayed ventricular repolarization must be conducted using the hERG assay [4].

Induced pluripotent stem (iPS) cells were recently established by transfecting murine and human fibroblasts with the transcription factors Oct3/4, Sox2, Klf4, and c-Myc, which are expressed at high levels in embryonic stem (ES) cells [5–7]. In regard to drug discovery, hiPS cells should make it easier to generate panels of cell lines that more closely reflect the genetic diversity of a population. As there are several genetic disorders known to affect the heart, such as familial cardiomyopathy, familial lethal arrhythmias, and congenital heart diseases, it is necessary to examine the development, pathogenesis, and physiologic characteristics of the hereditarily diseased human cardiomyocytes. In these respects, hiPS-derived cardiomyocytes (hiPS-CMs) confer significant advantages, since it is difficult to obtain living diseased cells from patients for the purposes of drug screening and analyses. In neurodegenerative diseases such as amyotrophic lateral sclerosis, Parkinson disease, and spinal muscular atrophy, patient-specific iPS cells have already been established [8–10]. To date, there has been no report on the establishment of *in vitro* models using hiPS-CMs for drug screening.

Multi electrode arrays (MEAs) enable measurement of the surface electrogenic activities of cell clusters. MEAs are easy to operate and can be adapted to automatic high-throughput systems. In addition, MEAs permit stable and long-duration recordings, which

* Corresponding author. Address: Department of Regenerative Medicine and Advanced Cardiac Therapeutics, Keio University, 35 Shinanomachi, Shinjuku-ku, Tokyo 160-8582, Japan. Fax: +81 3 5363 3875.
E-mail address: kfukuda@sc.itc.keio.ac.jp (K. Fukuda).
[1] These authors have contributed equally to this work.

0006-291X/$ - see front matter © 2009 Elsevier Inc. All rights reserved.
doi:10.1016/j.bbrc.2009.05.073

are necessary to evaluate the relationships between dose-dependency and the induction of side-effects for new drugs. The washing out of drugs from the external solution leads to the recovery of the field potential (FP) waveform almost to the baseline observed before drug application, which means that this system can be used to test the reproducibility of pharmacologic effects and that the effects of several drugs can be examined using the same preparation.

In the present study, we examined the electrophysiologic capacity of hiPS-CMs in responding to several cardiac drugs and measured the responsiveness of hiPS-CMs to representative sodium, calcium, and potassium ion channel blockers. This is the first report to validate the concept of drug screening using hiPS-CMs together with the MEA system.

Materials and methods

Cell culturing. The hiPS cell line 201B7, into which Oct3/4, Sox2, Klf4, and c-Myc were retrovirally transfected [5], was maintained in the undifferentiated state by co-culturing with a mitomycin C-inactivated mouse embryonic fibroblast (MEF) feeder layer in DMEM/F12 medium (Invitrogen) that was supplemented with 20% Knock-out Serum Replacement (KSR), 1 mM L-glutamine, 1 mM non-essential amino acids, 0.1 mM β-mercaptoethanol, and 4 ng/ml basic fibroblast growth factor (bFGF). The hiPS cell culture medium was changed daily and the cells were passaged every 5–6 days.

Embryoid body (EB) formation and cardiac differentiation. The hiPS colonies were dispersed into cell aggregates that contained 2000–5000 cells using CTK dissociation solution [11]. For differentiation, hiPS colonies of appropriate size were chosen using a combination of 40 μm and 100 μm cell strainers (Becton–Dickinson), which also facilitated the complete removal of feeder cells. The cell aggregates were cultured in suspension in ultra-low attachment cell culture dishes in hiPS differentiation medium (DMEM/F12 supplemented with 20% FBS, 1 mM L-glutamine, 1 mM non-essential amino acids, and 0.1 mM β-mercaptoethanol). The EBs were incubated at 37 °C in 5% CO_2. During differentiation, the medium was replaced every 3–4 days. Some of the EBs began to beat spontaneously 14–15 days after differentiation. The beating EBs were selected for analysis.

Reverse transcription-polymerase chain reaction (RT-PCR). Total RNA samples were isolated from undifferentiated hiPS cells (Day 0) and from EBs (Day 28 of differentiation) using the RNeasy kit and treatment with RNase-free DNase I (Qiagen), according to the manufacturer's instructions. NA concentration and purity were determined using the ND-1000 spectrophotometer (Nanodrop®). The cDNA was synthesized using the Superscript First-Strand Synthesis System (Invitrogen). PCR was performed with KOD Plus (Toyobo, Japan). The primers used in the PCR are listed in Table 1.

Immunostaining. Several beating EBs were mechanically excised and dissociated using collagenase IV and trypsin. Dissociated cells were seeded into fibronectin-coated dishes. The cells were fixed in 4% paraformaldehyde for 5 min at 4 °C and subsequently permeabilized with 0.1% Triton X-100 (Sigma–Aldrich) at room temperature. After pretreatment with ImmunoBlock (KN001; Dainippon Sumitomo Pharma), the cells were incubated at 4 °C overnight with the primary antibodies diluted in Tris buffer. The primary antibodies were: mouse monoclonal anti-α actinin (1:200 dilution; Sigma–Aldrich), anti-myosin heavy chain (MF20) (1:100; Developmental Studies Hybridoma Bank), and anti-muscle tropomyosin (1:100; Developmental Studies Hybridoma Bank); goat polyclonal anti-Nkx2.5 (1:50; Santa Cruz Biotechnology) and anti-GATA4 (1:50; Santa Cruz Biotechnology); and rabbit polyclonal anti-atrial natriuretic peptide (ANP) (1:200; Phoenix Pharmaceuticals). The fluorescent dye-conjugated secondary antibodies were applied to the cells for 30 min at room temperature. The secondary antibodies were Alexa Fluor 488-conjugated donkey anti-mouse IgG (H+L) (1:200; Invitrogen), Alexa Fluor 546-conjugated donkey anti-goat IgG (H+L) (1:200; Invitrogen), and TRITC-conjugated polyclonal swine anti-rabbit IgG (1:200; Dako Cytomation). Nuclei were stained with ToPro3 (Invitrogen), and the specimens were observed by confocal laser microscopy (LSM 510 META; Carl Zeiss).

Table 1
Oligonucleotide primers used for RT-PCR.

Target genes	Gene description	Primer sequence	AT (°C)	Number of cycles
SCN5A	Human sodium channel	Forward 5′-TGCTGAGTATGCCGACAAG-3′ Reverse 5′-GTTGATGCACCTCCCAAAT-3′	55	35
$Ca_v1.2$	L-type Ca^{2+} channel subunit	Forward 5′-TGGAAGCTCAGCTCCAACAG-3′ Reverse 5′-TCCTGGTAGGAGAGCATCTC-3′	55	35
KCNH2	Rapidly delayed rectifier K^+ channel	Forward 5′-CAGAGCCGTAAGTTCATC-3′ Reverse 5′-TCCTTCTCCATCACCACCTC-3′	55	35
GAPDH	Glyceraldehyde-3-phosphate dehydrogenase	Forward 5′-ACCACAGTCCATGCCATCAC-3′ Reverse 5′ TCCACCACCCTGTTGCTGTA 3′	60	35
β-Actin		Forward 5′-GACGAGGCCCAGAGCAAGAG-3′ Reverse 5′-ATCTCCTTCTGCATCCTGTC-3′	60	35
Oct3/4	Octamer-binding transcription factor 3	Forward 5′-CCTGGGGGTTCTATTTGGGA-3′ Reverse 5′-TTTGAATGCATGGGAGAGCC-3′	60	35
GATA4	Gata binding protein 4	Forward 5′-GGAGGAAGGCTCTCACTGCC-3′ Reverse 5′-GAGTGGGCCTCTCCTGTG-3′	60	35
Nkx2.5	NK2 transcription factor related, locus 5	Forward 5′-CGCCCTTCTCAGTCAAAGAC-3′ Reverse 5′-AGATCTTGACCTGCGTGGAC-3′	55	35
ANP	Atrial natriuretic peptide	Forward 5′-GAACCAGAGGGGAGAGACAGA-3′ Reverse 5′-CCCTCAGCTTGCTTTTTAGGAG-3′	60	35
MLC2a	Myosin light chain 2 atrial	Forward 5′-CCAACGTGGTTCTTCCAAC-3′ Reverse 5′-TCCTCCTCTGGGACACTCAC-3′	60	35
MLC2v	Myosin light chain 2 ventricular	Forward 5′-CAGAACAGGGATGGCTTCAT-3′ Reverse 5′-GGTCCGCTCCCTTAAGTTTC-3′	60	35
α-MHC	Cardiac alpha-myosin heavy chain	Forward 5′-AGGATCCTCTCAACGAGACT-3′ Reverse 5′-GTGATCAATGTCCAGAGAGC-3′	55	35
β-MHC	Cardiac beta-myosin heavy chain	Forward 5′-AGATGGATGCTGACCTGTCC-3′ Reverse 5′-CTCTTCCTCATGCCCTTCAC-3′	60	35

KCNH2: hERG, AT: annealing temperature.

Field potential recordings using the On-Chip MEA system. MEA chips were obtained from Photo Precision (Japan), ULVAC (Japan), and Alpha-MED Science (Japan). The MEA chips were coated with collagen type I-C (Nitta Gelatin, Osaka, Japan) or fibronectin (Sigma). Beating EBs were plated on the electrodes and incubated at 37 °C in a humidified atmosphere of 95% air and 5% CO_2 after the drug assay.

Field potential (FP) recordings of the beating EBs were performed using the On-Chip MEA system (Yasuda Laboratory, Tokyo, Japan) at a sampling rate of 10–100 kHz with low path filter of 2–10 kHz and high path filter of 0.1–100 Hz, and amplified by 100–50,000 using the NF amp (NF, Japan) [12]. All MEA measurements were performed at 37 °C. The signals were initially processed with the CellAD 2.0 software (DITEC, Japan), and the obtained data were subsequently analyzed with the OriginPro 8.0J and FlexPro 7.0 programs. Data for analysis were extracted from 2 min to 5 min of the obtained data.

E-4031, verapamil, quinidine, and isoproterenol (all from Sigma) were prepared as 0.1 mM, 1 mM, 10 mM, and 10 μM stock solutions in distilled water, respectively. These stock solutions were diluted to the required concentration in culture medium and applied to the test chip.

The protocol for the drug assay is described below. The medium on the test chip was exchanged for fresh medium, and then the FPs were recorded for 5 min. Subsequently, the drug was applied to the medium at 1–5% dilution and the FPs were measured for 5–10 min. Finally, washing out was performed, to exchange the medium three times per min, and 60–90 min after washout, the FPs were recorded for 5 min.

Results

Expression of cardiac marker genes in hiPS-CMs

Initially, we investigated whether the spontaneously beating cells possessed the characteristics of human cardiomyocytes. The expression levels of various cardiac marker genes were analyzed by RT-PCR (Fig. 1A). Oct3/4 was expressed in the undifferentiated hiPS cells, whereas it was not expressed after the hiPS cells differentiated. Cardiac transcription factors, e.g., Nkx2.5 and GATA4, and cardiac-specific proteins, e.g., the α- and β-myosin heavy chains (MHC), myosin light chains (MLC) 2a and 2v, and ANP, were detected in hiPS-derived EBs that contained spontaneously contracting cells.

We performed immunofluorescence staining to determine whether the spontaneously beating cells expressed cardiac marker proteins and structures (Fig. 1B–D). These cells displayed: (1) sarcomere formation, based on positive staining with antibodies directed against α-actinin, MHC, and tropomyosin; (2) nuclear expression of the cardiac-specific transcription factors Nkx2.5 and GATA4; and (3) the presence of ANP in the secretory granules surrounding the nuclei, which is a typical feature of cardiomyocytes. These findings indicate that hiPS cells differentiate into cardiomyocytes.

Expression of functional ion channels in hiPS-CMs

We investigated the levels of transcripts for cardiac ion channel genes by RT-PCR. The gene for the sodium channel α-subunit

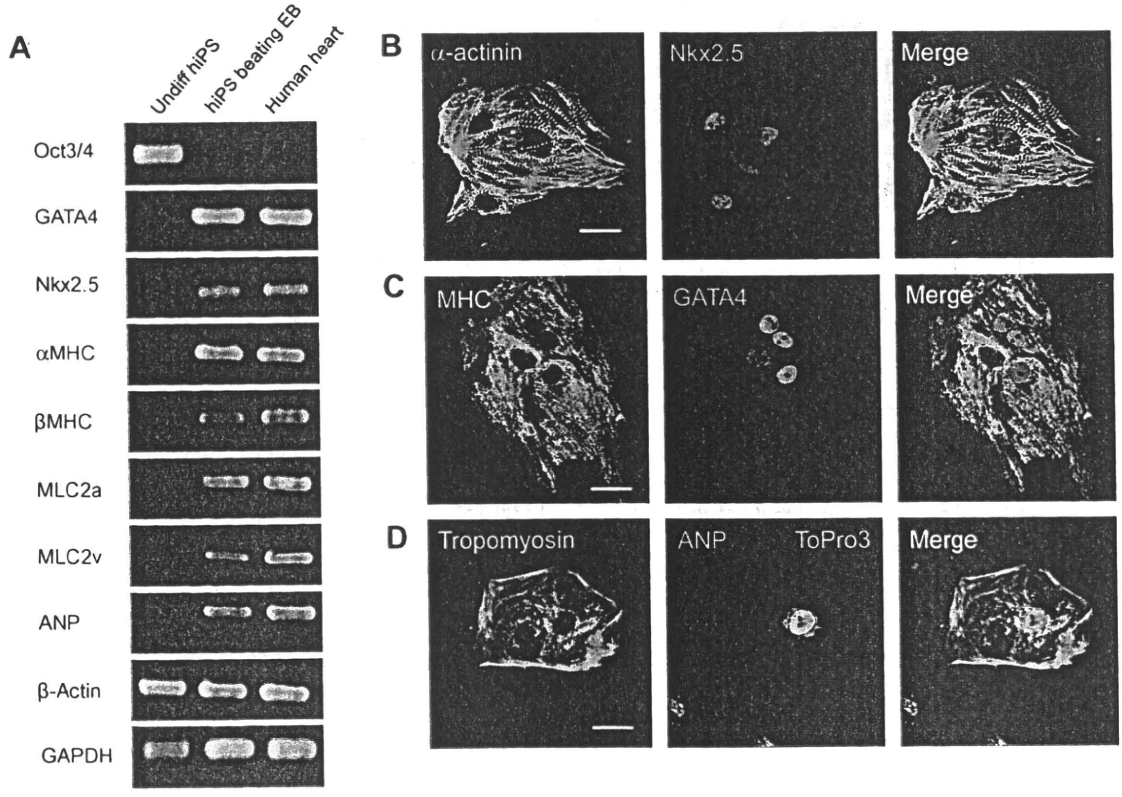

Fig. 1. Cardiomyocyte differentiation from human iPS cells. (A) Gene expression profiles of various cardiac markers and sarcomeric proteins. RT-PCR was performed on undifferentiated cells and differentiated cardiomyocytes. Human heart tissue was used as a positive control. Oct3/4, octamer-binding transcriptional factor 3/4; ANP, atrial natriuretic peptide; GATA4, GATA binding protein 4; Nkx2.5, NK2 transcription factor-related, locus 5; MHC, myosin heavy chain; MLC, myosin light chain. (B) Double-immunostaining for α-actinin (green) and Nkx2.5 (red). Right panel, merged image. (C) Double-immunostaining for MHC (green) and GATA4 (red). Right panel, merged image. (D) Double-immunostaining for tropomyosin (green) and ANP (red). Right panel, merged image with ToPro-3 (blue) staining of the nuclei. Scale bar, 10 μm (B–D).

SCN5A, which determines cardiac excitability and conduction velocity, was expressed in differentiated hiPS cells, but not in undifferentiated cells. Differentiated hiPS cells also expressed the genes for $Ca_v1.2$, which is an L-type Ca^{2+} channel α-subunit that contributes to cardiac contraction, and KCNH2 (hERG), which is a rapidly activating delayed rectifier K^+ channel (I_{Kr}) that contributes to AP repolarization. The genes for these ion channels were not expressed in the undifferentiated hiPS cells (Fig. 2A).

To characterize the electrophysiological properties of hiPS-CMs, the FPs of the spontaneously beating EBs were recorded using the On-Chip MEA system, as previously described [12]. First, we investigated the effects of ion channel-specific inhibitors on the FP waveform, to determine whether the expressed channels were functional. As shown in Fig. 2B, the sodium channel inhibitor quinidine dose-dependently and reversibly attenuated the length of time required for the decline in voltage from the baseline to the first negative peak (FP amplitude), which reflects the AP upstroke, without significant changes in the spontaneous beating rate. These findings indicate that a functional sodium channel is expressed in the hiPS-CMs. Next, we tested the effect of the calcium channel blocker verapamil on the FP waveform. Verapamil dose-dependently shortened the length of time from the first negative peak (open triangle) to the first positive peak (closed triangle) (FPD), which was consistent with the effect of calcium channel inhibition on AP duration (Fig. 2C). Disruption of potassium channels might lead to prolongation of cardiac repolarization, potentially leading to life-threatening arrhythmias, e.g., TdP and ventricular tachycardia. Therefore, we examined the effect of the I_{Kr} blocker E-4031 on the FP waveform. E-4031 dose-dependently and reversibly prolonged the FPD (Fig. 2D). These results suggest that the main cardiac deporalizing and repolarizing ion channels are functionally expressed in the hiPS-CMs.

β-Adrenergic modulation of spontaneously beating hiPS-CMs

To study the response to adrenergic stimulation, isoproterenol was added to the cells. Isoproterenol dose-dependently increased the beating frequency of the cardiomyocytes, as compared with the baseline frequency, indicating an intact and coupled β-adrenergic signaling cascade (Fig. 3).

Discussion

Drug-induced prolongation of the electrocardiographic QT interval is associated with an increased risk of a serious ventricular arrhythmia, such as TdP. To avoid this problem, binding assays with radiolabeled drugs and recombinant hERGs are used. However, these are typically applied to the late developing candidates

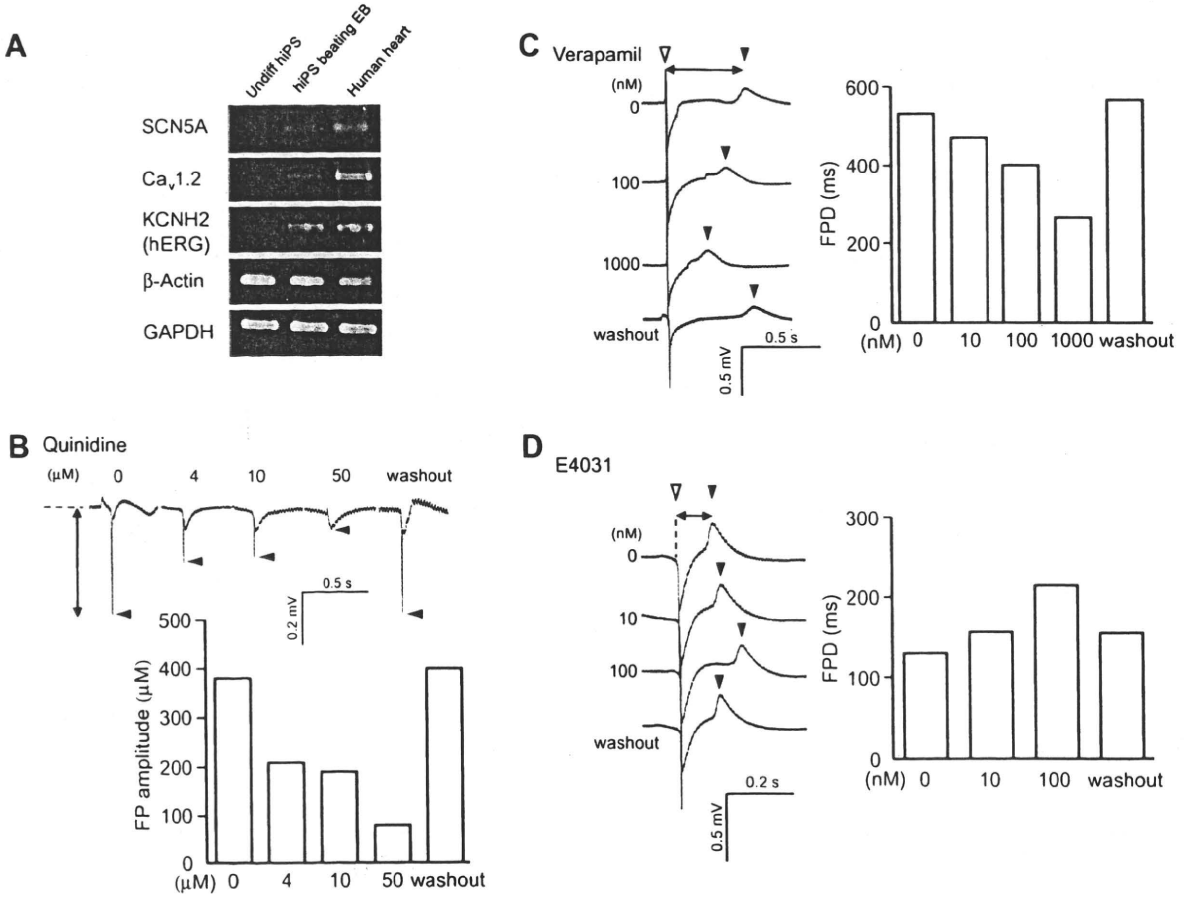

Fig. 2. Functional ion channel expression in human iPS-derived cardiomyocytes. (A) Gene expression profiles of various ion channels. RT-PCR was performed on undifferentiated cells and differentiated cardiomyocytes. Human heart tissue was used as a positive control. (B) Effect of quinidine on the field potential (FP) waveform recorded for the hiPS-derived beating EBs. The upper traces show representative FPs for the various concentrations of quinidine and after washout. The first negative peak of the FP (closed triangle) reflects an action potential upstroke. The lower graph summarizes the changes in FP caused by quinidine. (C) Effect of verapamil on the FP waveform recorded for hiPS-derived beating EBs. The left traces show representative FPs for the various concentrations of verapamil and after washout. The time period from the first negative peak (open triangle) to the first positive peak (closed triangle) (FPD, arrow) reflects the action potential duration. The right graph shows a summary of the changes in FPD caused by verapamil. (D) Effect of E-4031 on the FP waveform recorded for the hiPS-derived beating EBs. The left traces are representative FPs for various concentrations of E-4031 and after washout. The right graph shows a summary of the changes in FPD caused by E-4031.